Halsey, N., Marlowe, D. E., Mitchell, R. A., Mordfin, L., Non-metallic antenna-support materials pultruded rods for antenna guys, catenaries and communications structures, AFML-TR-76-42, 126 pages (Air Force Materials Laboratory, Wright-Patterson Air Force Base, OH, May 1976).

NBSIR 75-684

16685

AFML-TR-76-42

NON-METALLIC ANTENNA-SUPPORT MATERIALS PULTRUDED RODS FOR ANTENNA GUYS, CATENARIES AND COMMUNICATIONS STRUCTURES

INSTITUTE FOR BASIC STANDARDS
NATIONAL BUREAU OF STANDARDS
WASHINGTON, D. C. 20234

MAY 1976

TECHNICAL REPORT AFML-TR-76-42
FINAL REPORT FOR PERIOD OCTOBER 1971 - OCTOBER 1974

Approved for public release; distribution unlimited

AIR FORCE MATERIALS LABORATORY
AIR FORCE WRIGHT AERONAUTICAL LABORATORIES
AIR FORCE SYSTEMS COMMAND
WRIGHT-PATTERSON AIR FORCE BASE, OHIO 45433

NOTICE

When Government drawings, specifications, or other data are used for any purpose other than in connection with a definitely related Government procurement operation, the United States Government thereby incurs no responsibility nor any obligation whatsoever; and the fact that the Government may have formulated, furnished, or in any way supplied the said drawings, specifications, or other data, is not to be regarded by implication or otherwise as in any manner licensing the holder or any other person or corporation, or conveying any rights or permission to manufacture, use, or sell any patented invention that may in any way be related thereto.

This final report was submitted by the National Bureau of Standards, Washington, D.C. 20234, under contract F33615-72-M-5000, Job Order 73810663, with the Air Force Materials Laboratory, Wright-Patterson Air Force Base, Ohio. Mr. John R. Rhodehamel, AFML/MXE, was the Laboratory Project Monitor.

This report has been reviewed and cleared for open publication and/or public release by the appropriate Office of Information (OI) in accordance with AFR 190-17 and DODD 5230.9. There is no objection to unlimited distribution of this report to the public at large, or by DDC to the National Technical Information Service (NTIS).

This technical report has been reviewed and is approved for publication.

John R. Rhodehamel
JOHN R. RHODEHAMEL
Project Monitor

Edward J. Morrisey
EDWARD MORRISEY
Supervisor

FOR THE COMMANDER

Albert Olevitch
ALBERT OLEVITCH
Chief, Materials Engineering Branch
Materials Support Division

621082

Copies of this report should not be returned unless otherwise required by security considerations, contractual obligations, or notice on a special document.

FOREWORD

This final report was submitted by the National Bureau of Standards, Washington, D.C. 20234, under contract F33615-72-M-5000, Job Order 73810663, with the Air Force Materials Laboratory, Wright-Patterson Air Force Base, Ohio. Mr. John R. Rhodehamel, AFML/MXE, was the Laboratory Project Monitor.

The effort was over the period of October 1971 through October 1974. The authors, Messrs. N. Halsey, D. E. Marlowe, R. A. Mitchell and L. Mordfin were responsible for the program direction.

This report was submitted by the authors in May 1976.

TABLE OF CONTENTS

TABLE OF CONTENTS
(CONTINUED)

LIST OF ILLUSTRATIONS

LIST OF TABLES

LIST OF TABLES
(CONTINUED)

SECTION I

INTRODUCTION

Fiber-reinforced-plastic (FRP) rod and rope materials constitute one of the more interesting and valuable -- although lesser known -- products of composite materials technology. These products are most commonly fabricated from unidirectional glass fiber roving and a thermosetting plastic matrix by a process called pultrusion. They are strong, lightweight, nonconducting, corrosion resisting and comparatively inexpensive. This combination of properties has led to the use of these products in a variety of applications where steel wire rope had previously been employed almost exclusively. In terms of total volume, the largest application has been in communications towers and arrays, wherein the use of non-metallic rod and rope as guys and catenaries has reduced corona and maintenance problems and permitted elimination of the large, expensive, ceramic insulators which are required when steel wire rope is used.

As frequently happens when promising new products are developed, the rod and rope were introduced into service before they were adequately characterized and without the benefit of carefully compiled design data. The result has been the occurrence of failures in several field installations. Fortunately, however, most applications have performed satisfactorily. Some of the reported failures have involved arc tracking and flashover damage, and burning, in intense electromagnetic fields. Most of the other reported failures were apparently mechanical although environmental effects were probably involved. Rope-type guys and catenaries have failed, at locations apart from their fittings by a progressive strand-by-strand breakage. The cause of these failures is unknown but opinions that have been advanced include undetected damage incurred during installation, wind-induced rubbing of adjacent strands, and strength degradation due to ultraviolet exposure. In the case of rod materials, failures have usually entailed splitting or delamination that progressed along the rod at a slight inclination to the longitudinal axis.

Lengthwise splitting of rods has been observed to emanate from localized surface defects. Such defects may be severe notches or gouges from damage introduced during handling, or they may be thin, deep transverse cracks. Some of these transverse cracks are particularly interesting because, prior to splitting, they appear only as barely visible hairlines on the surface of the rod. The surfaces of the cracks are very smooth. Unpublished research at NBS has verified that these cracks can result from a two-state dynamic loading sequence. It is also believed that lengthwise splitting can result from the fact that the rods are sometimes bowed, rather than straight, when installed. In this circumstance the applied tensile forces create lengthwise shearing stresses which may exceed the low shear strength of the product.

Although the causes of mechanical failure in these materials are apparently many and varied, at least one generalization can be made. Most mechanical failures on non-metallic antenna support materials have occurred after a period of service, ranging from months to years, during which the materials have been under tension in a moist environment. With this as a point of departure, the National Bureau of Standards embarked upon a three-year program to develop a new non-metallic fiber-reinforced-plastic rod material which would exhibit superior mechanical properties and greater resistance to moisture. The program called for the development to be accomplished through (1) the selection of potential improvements in the manufacturing process and in the constituent materials; (2) the procurement of experimental materials manufactured in accordance with these potential improvements; and (3) the subsequent evaluation of these materials. The evaluations were based primarily upon two types of mechanical tests: tensile tests at normal and high rates of loading, and stress-rupture tests at 160 and 200°F (71 and 93°C) under saturated humidity conditions. The results of the stress-rupture tests, when performed on a variety of materials, were considered to be indicative of the relative weatherabilities of the materials.

This program was carried out in the Engineering Mechanics Section of NBS under the sponsorship and with the financial assistance of the Air Force Materials Laboratory. Laboratory efforts were in response to an Air Force Technical Need (TN-ESD 26-70-01). This Category I program required that a data base be established for (future) antenna structures design. The authors gratefully acknowledge the valuable contributions of Mrs. Ruth M. Woolley, Mr. Oscar O. Owens and Mr. Raymond G. Russell of the Engineering Mechanics Section, NBS, and of Dr. Fred A. Yeoman, Mr. John S. Hudock and Mrs. Donna K. Nowakowski of the Westinghouse Electric Corporation.

Since the English system of units is used almost exclusively by the American manufacturers and users of non-metallic antenna-support materials at this time, these units have been employed in this report. In each instance, however, the English units are followed by their metric (SI) equivalents in parentheses. Factors for converting between the two systems of units may be found in the Standard Metric Practice Guide (ASTM Designation E 380-72) which is available from the American Society for Testing and Materials, 1916 Race Street, Philadelphia, Pa. 19103.

SECTION II

EVALUATION OF EXISTING FRP ROD PRODUCTS

1. THE PULTRUSION PROCESS

A survey of commercial FRP rod and rope manufacturers was carried out to identify the critical features of the pultrusion process as it is used for the manufacture of FRP materials. Although the process was comparatively obscure at the start of this program, recent publications (1, 2, 3) suggest that it is rapidly becoming more widely known and used. The basic features of this process are reviewed here. Figure 1 is a schematic of the process which illustrates several features that are common to most manufacturers. It should be noted, however, that no two manufacturers were surveyed whose processes were identical.

On the left of the figure, glass rovings are drawn from a creel in which are mounted dozens of bales or spools of roving. The rovings are guided down into the resin tank where the individual fibers are wetted with the matrix resin. Following this, the impregnated mass is drawn through one or more guides and bushings which give the material its desired cylindrical shape. Finally, the rod is cured in a heated die system.

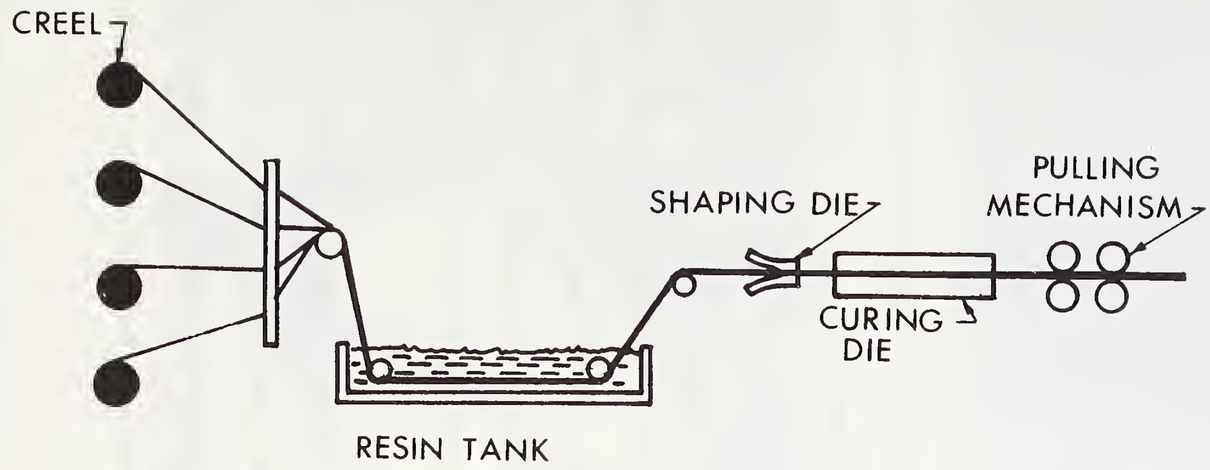

Figure 1 - Schematic Representation of the Pultrusion Process

On the right of the figure is the pulling mechanism which gives the pultrusion process its name and which supplies the considerable force that is required. The final product is either cut to desired lengths or coiled and allowed to cool.

2. DEFICIENCIES IN EXISTING PULTRUDED PRODUCTS

Commercially available glass FRP rods from five different pultrusion manufacturers were examined to identify those product characteristics which could be responsible for the premature mechanical failures that have been experienced in antenna-support applications. Six such deficiencies were found to be present, in varying degrees, in all of the products. These deficiencies, which appeared to be correctible by appropriate modifications of the manufacturing process, are described here together with the inspection procedures which were used to identify them.

Microscopic examinations of cross sections of an FRP rod provide a simple means for assessing the uniformity of the distribution of fibers in the rod. Photomicrographs, such as those shown in Figure 2, clearly reveal that the fibers are not uniformly distributed throughout the cross section. Instead, they appear to be bunched together in clusters with resin-rich areas between them. It is speculated that each cluster corresponds to the ends of a single roving.

When a glass FRP rod is properly tested in tension, such that failure initiates in the free length of the rod, the fracture generally causes the fibers to broom out in a rather explosive fashion. Examination of the fibers in such cases reveals that many do not appear to be wetted by the resin.

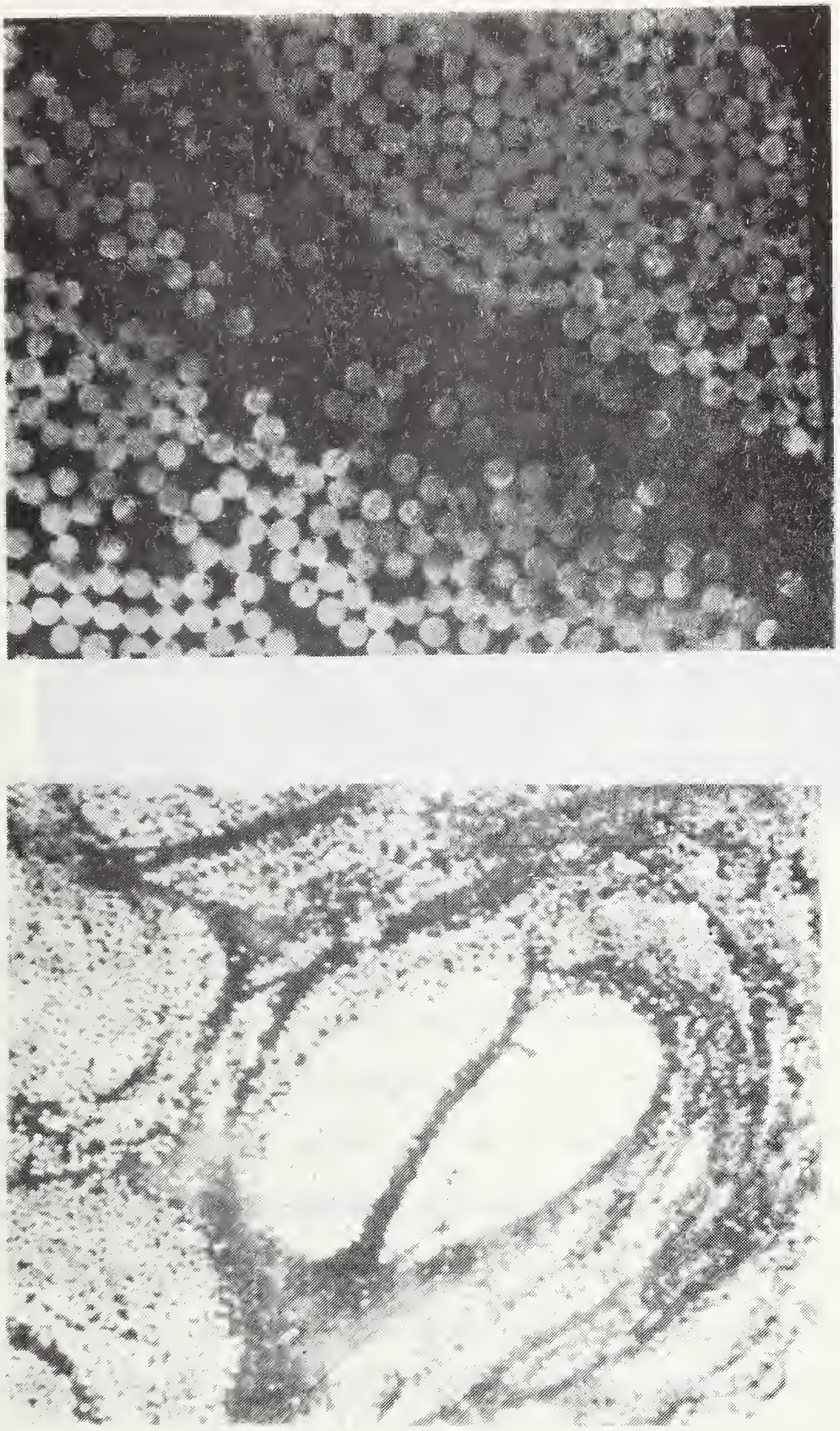

Figure 2 - Photomicrographs of Cross Section of 1/2-in (13-mm) Diameter Pultruded rod. X340 Magnification (above) and X70 Magnification (below)

(continued)

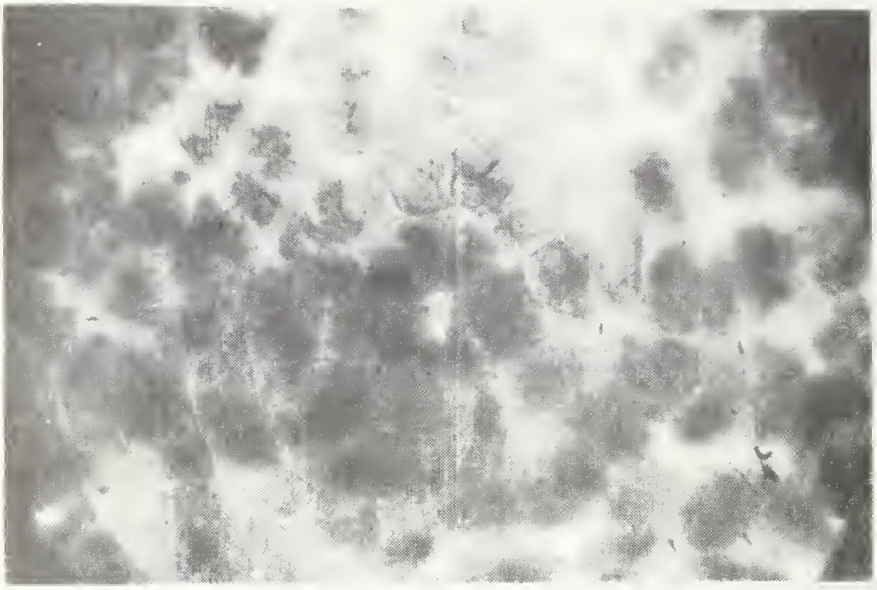

Figure 2 (continued) - X9 Magnification

Photomicrographs made under high magnification frequently show apparent voids adjacent to individual fibers. This tends to confirm the above observation regarding incomplete wetting. However, apparent microscopic voids are also occasionally observed in the matrix at locations apart from fibers. It is speculated that these voids may be created by volatilization of one or more components of the resin system under the heat of the curing operation.

Careful examination of the surface of an uncoated FRP rod occasionally permits the paths of individual fibers to be traced for some distance before the fibers descend into the interior of the rod. Such examinations reveal that the fibers are not straight but follow a rather wavy path. Obviously, this condition is not conducive to achieving a uniform distribution of load among the fibers in a tensile application.

Further examination of surface characteristics, particularly on fractured rods, reveals that even when the fibers are straight they are frequently not parallel to the axis of the rod. Deviations of 10° to 20° are not uncommon. In this situation the potential tensile strengths of the rods cannot be fully realized.

Hardness measurements on FRP rods have been made, both before and after post-curing operations. In all cases the post cure produced an increase in hardness. This is taken to mean that the rods, in the as-received condition, were not fully cured since a fully cured rod should exhibit no significant increase in hardness during post curing.

SECTION III

TEST METHODS FOR EXPERIMENTAL MATERIALS

The program for the development of improved FRP rod materials called for the manufacture of a series of experimental rods, to be discussed later. The most critical mechanical properties of the experimental rod materials, namely, strength and weatherability, were evaluated by means of room-temperature tensile tests, at both normal and high loading rates, and by stress-rupture tests, at 160 and 200°F (71 and 93°C), under saturated humidity conditions. In addition, a variety of supplementary test methods and measurement techniques was used to study other physical characteristics of the experimental rod materials such as dimensional uniformity, resin content, degree of fiber wetting, degree of cure and transverse tensile strength.

1. TENSILE TESTS

The tensile tests at normal loading rates were performed in a 100,000-lbf (450-kN) capacity, horizontal, hydraulic, universal testing machine [4]. A crosshead speed of 0.75 in/min (0.32 mm/s) was used.

The tensile tests at high loading rates were carried out in a 50000-lbf (220-kN) capacity, closed loop, electrohydraulic testing machine [4]. A calibrated load cell in series with the test specimen was used to measure load, and the load-time trace for each test was recorded with a calibrated storage oscilloscope. The crosshead speed in these tests was measured using an LVDT extensometer and was found to be approximately 300 in/min (130 mm/s).

The most difficult problem to be overcome, in measuring the tensile strengths of unidirectionally reinforced rods, is avoiding premature failures of the rods that initiate in the end fittings. It has been established [5] that commercially available end fittings for FRP rod and rope are not generally satisfactory for this purpose. Consequently, a concerted effort was made to develop new end fittings which could be used to measure the full tensile strengths of the rod materials studied in this program. This development effort is described in Section 4 of this report.

2. STRESS-RUPTURE TESTS

The stress-rupture tests were performed in six creep-testing machines that were designed and assembled for this task. Each of these machines has a rated capacity of 30000 lbf (130 kN), which is applied by dead weights acting through a 100:1 compound lever system. Specimens up to 9 ft (3 m) long, including the end fittings, can be accommodated. The overall height and length of each machine are approximately 7 ft (2 m) and 12 ft (4 m), respectively.

Each creep-testing machine was equipped with an environmental test chamber for providing the required temperature and humidity conditions. The chambers are cylindrical in shape, consisting primarily of a 10-in (0.25-m) diameter asbestos-cement pipe, 4 ft (1.2 m) long, with transparent plastic windows at the ends. Each chamber contains a brass tube which extends nearly the full length of the chamber. The purpose of the tube was to provide a more uniform temperature distribution on the specimen, which passed concentrically through the tube. The ends of the specimen, including the end fittings and the pull rods, remained outside of the chamber.

Heat was supplied to each chamber by twelve quartz-tube infrared lamps which surround the brass tube. Each lamp has a capacity of 500W at 120V. The temperature distribution in the chamber was adjusted by regulating the power to the lamps. The test temperature was maintained with a temperature controller.

Each chamber was furnished with an air-powered mist generator to provide the required saturated humidity conditions. The rate of water consumption was adjusted by regulating the air-flow rate to maintain a light film of condensation on the windows of the chamber.

3. RESIN CONTENT

The determination of the resin content of glass FRP rods was made by means of a burn-out test similar in principle to the ASTM ignition loss test [6]. This test involves the use of a continuous-reading scale which is enclosed in a muffle furnace. The furnace temperature is set at a value at which the organic resin matrix material is completely decomposed to volatiles. The difference between the original weight of a sample and the minimum weight achieved during heating is considered to be the resin content.

4. DIMENSIONAL UNIFORMITY

Measurements of the average diameter, the length, and the weight (mass) of several sections of each FRP rod material were made. The densities [7] and the weights (masses) per unit length were calculated. These determinations provide an indication of the uniformity of the product.

5. FIBER WETTING

An indirect indication of the degree of fiber wetting was obtained by measuring the corona inception voltage on rod samples which had been saturated with water. This approach was based on the premise that absorbed water will migrate to fiber-resin interfaces which are not thoroughly adhered. The following test procedure [8] was adopted for the experimental FRP rod materials:

(1) Cut a 1/2-in (13-mm) long specimen from 1/2-in (13-mm) diameter rod, with the ends smooth and parallel.

(2) Boil the specimen in distilled water for 2 h.

(3) Measure the electrical breakdown voltage across the parallel faces within 15 min after removal from the water, as follows:

  (a) Mount the specimen between 1-in (25-mm) diameter electrodes in an oil bath.

  (b) Raise the voltage across the specimen from 0 to 15 kV at a rate of 0.5 kV/s.

  (c) Hold the voltage at 15 kV for 1 min. If failure occurs within this interval, record the failure voltage as 15 kV.

  (d) Increase the voltage further at a rate of 0.5 kV/s to breakdown voltage. (The maximum voltage from the available equipment was 50 kV.)

6. DEGREE OF CURE

Rockwell hardness measurements were made on FRP materials as an indication of the degree of cure of the resin. For this purpose Procedure A of ASTM Designation D785-65 [9] was used. Samples were removed from several locations along the length of a rod. A minimum sample length of 2 in (50 mm) was established to enable multiple measurements to be made on the same sample. Not less than five measurements were made on the cylindrical surface of each sample. Three of these were made on a single generator line. The other two measurements were made on a second generator line, 90^{o} from the first line, at points intermediate to the first three test sites.

7. TRANSVERSE TENSILE STRENGTH

A measure of the transverse tensile strength of FRP rod was obtained by means of a diametral compression test. In this well-known test method for brittle materials [10] a cylindrical disk-shaped specimen is compressed diametrically between two flat platens. Under the proper conditions [11] the test culminates in a tensile fracture along the loaded diameter, and the transverse tensile strength σ_t of the rod is calculated from the relation

$$\sigma_t = \frac{2P}{\pi D t}$$

where P is the compressive load at fracture, D is the diameter of the disk and t is its thickness. These transverse tensile strength measurements are believed to represent some combination of the tensile strengths of the resin matrix material and the fiber/matrix bond.

Disk specimens, approximately 1/4 in (6 mm) thick, were sliced from 1/2-in (13-mm) diameter FRP rods using a water-cooled, diamond cutoff saw. Care was taken during this cutting process to prevent fraying of the edges. The coolant was carefully blotted from the disks which were then allowed to dry, under ambient laboratory conditions, for at least 24 h prior to testing. The diameter and thickness of each specimen was measured, and the specimen was mounted, on edge, in a compression subpress [12] and loaded to fracture in a universal testing machine.

SECTION IV

DEVELOPMENT OF IMPROVED END FITTINGS

In this task, laboratory prototypes of two new end fittings were developed which are superior to a variety of commercial end fittings in terms of their capability to approach the full strength of FRP rod in a tensile test. While the development of these fittings was completed in the present program, much of the basic work which went into the development was initiated or pursued in prior studies performed in this laboratory [5, 13]. These prior studies were carried out under the sponsorship and with the financial assistance of the Army Electronics Command, the Coast Guard, the Naval Facilities Engineering Command, Rome Air Development Center (USAF), the United States Information Agency and the National Bureau of Standards.

The basic approach to the development of improved end fittings consisted of an analytical parameter study of the problem and an experimental evaluation of trial prototype designs, which were pursued concurrently. The analytical study involved the axisymmetric, finite-element stress analysis of a broad class of end connections consisting of a metal sleeve joined to the FRP rod with a polymeric potting material. The experimental study involved the fabrication and tensile testing of prototype end fittings employing several different gripping concepts. An important aspect of this parallel analytical and experimental approach was the free transfer of newly developed information from one study to the other. Some aspects of the analytical study are reported in greater detail elsewhere [14].

1. ANALYTICAL STUDY

A new computer program was developed for the axisymmetric finite-element stress analysis of end connections. The basic finite-element formulation used [15] had been developed for the case of isotropic elastic materials. That earlier formulation was modified in the end-fitting analysis in accordance with the assumption that the FRP rod is homogeneous and transversely isotropic as defined by five independent elastic constants. The metal sleeve and the potting compound were assumed to be isotropic elastic.

Figure 3 shows a representative finite-element analysis mesh for one general class of end connections. In this case, the metal sleeve is conically tapered, and the outer end of the FRP rod is slit into quarters and spread with a conical metal wedge. Where the rod is spread by the wedge, the elastic constants for the region occupied by the spread rod were recomputed according to the volume fractions of rod material and potting compound.

The linear elastic finite-element computer model was used in a parameter study of the general class of end fittings represented schematically in Figure 4. The numerals in the figure denote the eight variable parameters studied. Parameters 4 and 5 are the elastic moduli of the two potting compounds indicated.

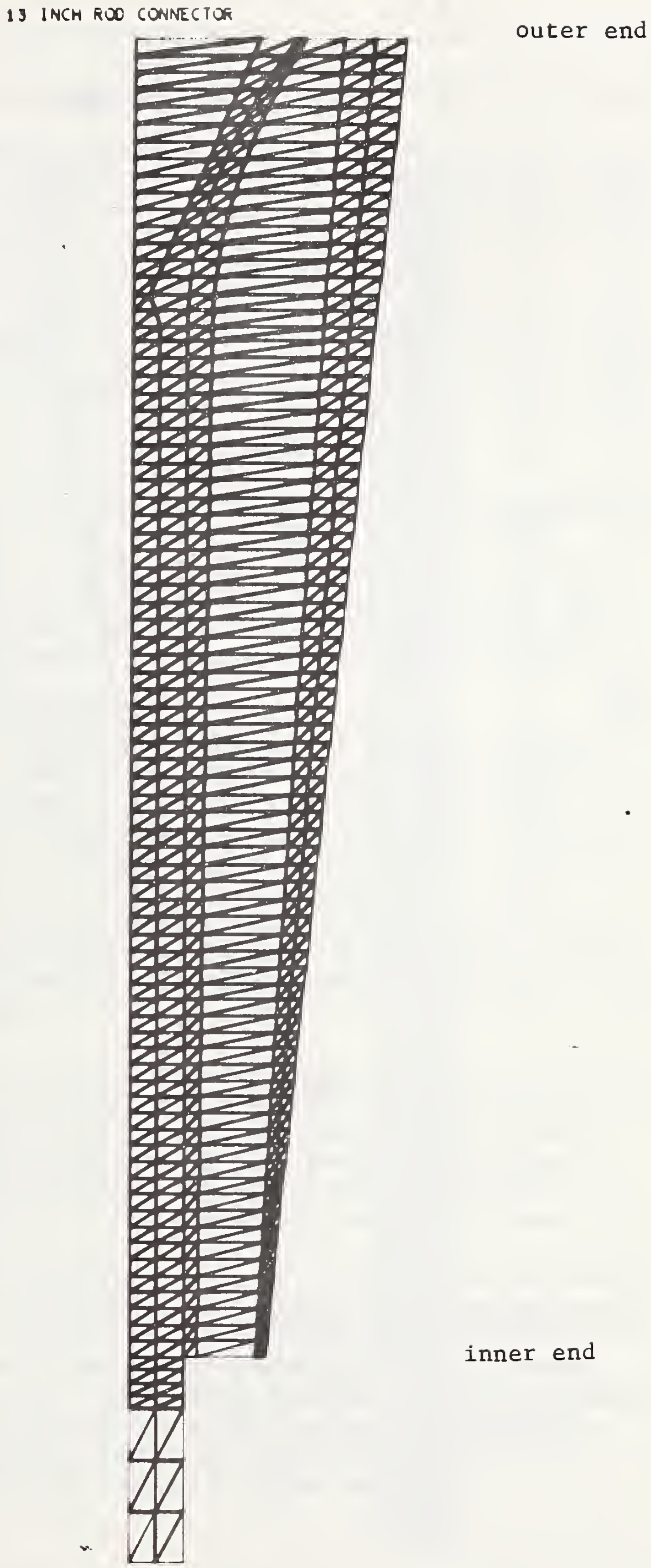

Figure 3 - Representative Finite-Element Mesh for One General Class of End Fittings

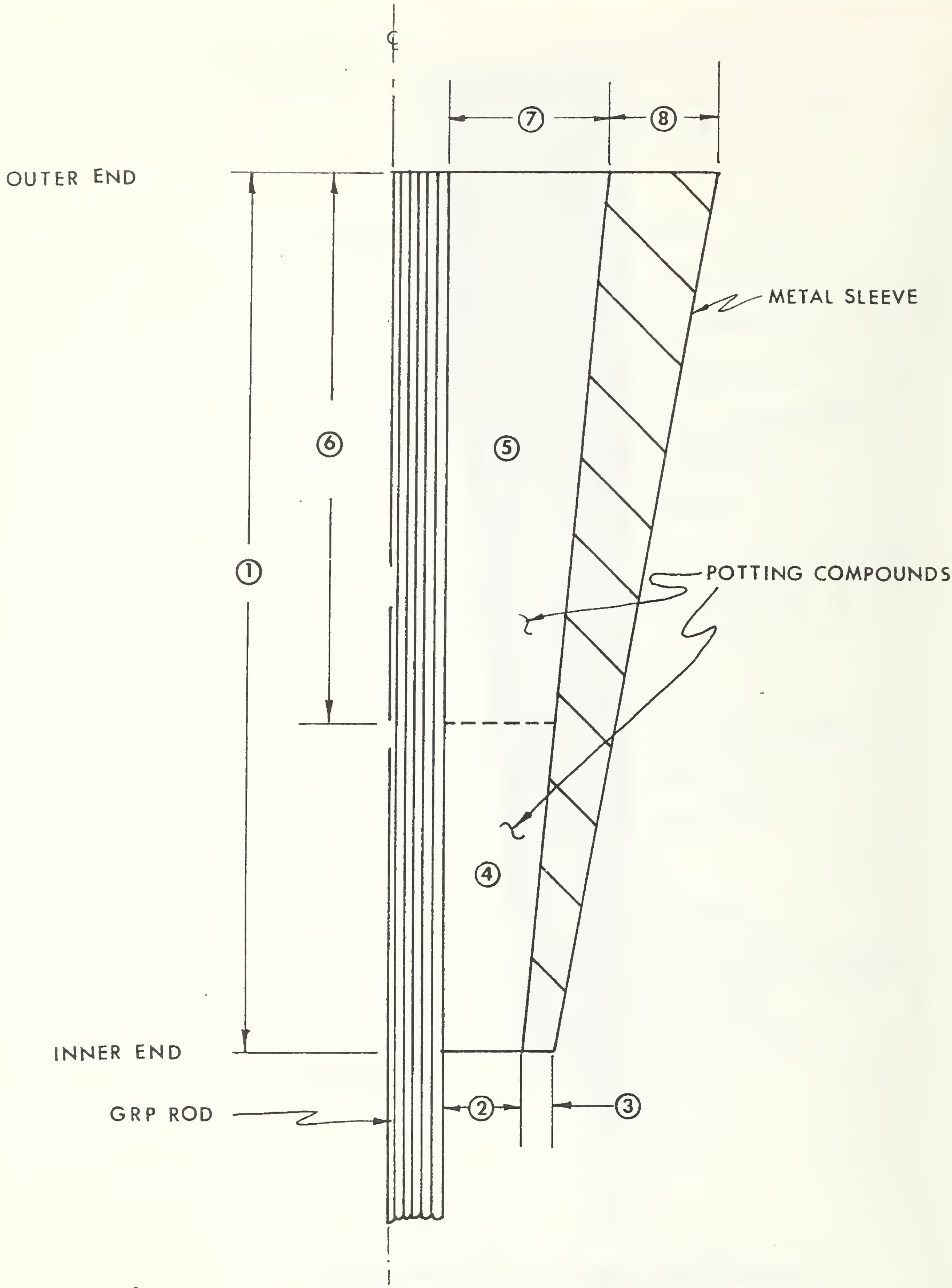

Figure 4 - Parameters for One General Class of End Fittings

It was assumed that the critical component of stress, with respect to tensile strength, is the peak bond-shear stress at the interface between the rod and the potting compound. This assumption was based on the fact that rod pullout was the most common failure mode observed in tensile tests of this class of fitting.

The analyses were carried out for a 1/2-in (13-mm) diameter FRP rod. The assumed properties of the metal sleeve and the conical wedge (not shown) were those of 7075-T6 aluminum alloy.

The general indications for the eight parameters studied are:

1. End-fitting length.--Within the range of 6 to 16 in (0.15 to 0.41 m), greater length results in significantly smaller peak bond-shear stress, but the rate of change of peak stress decreases as length increases.

2. Potting thickness at inner end of fitting.--Within the range of 0.24 to 0.48 in (6 to 12 mm), greater thickness results in significantly smaller peak bond-shear stress, but the rate of change of stress decreases as thickness increases.

3. Sleeve thickness at inner end of fitting.--Within the range of 0.02 to 0.25 in (0.5 to 6.4 mm), greater thickness results in slightly greater peak bond-shear stress.

4. Elastic modulus of inner potting compound.--Within the range of 40000 to 316000 lbf/in (0.28 to 2.18 GPa) greater stiffness of potting compound results in significantly greater peak bond-shear stresses. This is true whether a single potting compound or a combination of two different compounds is used.

5 & 6. Elastic modulus and length of outer potting compound.--A combination of two potting compounds having different elastic moduli produces two bond-shear stress peaks (one at the inner end of each potting compound). If Parameters 4, 5 and 6 are proportioned so as to make the two stress peaks approximately equal, the peak stress is significantly less than for the case of a single potting material.

7 & 8. Potting thickness and sleeve thickness at the outer end of the fitting.--Parameters 7 and 8 have a relatively small direct influence on the peak bond-shear stress.

The two most significant findings of this parameter study are:

1. The potting compound should have a relatively low modulus of elasticity, i.e., it should be flexible.

2. The potting compound layer should be relatively thick. A ratio of rod diameter to layer thickness of not less than 4 may be used.

Both of these findings appear to be entirely logical but they were not intuitively obvious prior to the parameter study. In particular, it is known that adhesives with high bond strengths generally have relatively high moduli of elasticity, and that adhesives generally exhibit higher bond strengths when applied in thin layers. However, the parameter study showed that a flexible, thick potting compound allows the tensile load to be transferred from the fitting to the rod gradually, over a long length, without developing a high peak bond-shear stress at the inner end of the fitting. Thus, a flexible, thick potting compound performs better in this application than a stiff, thin potting compound which may have a greater bond strength.

2. SELECTION OF POTTING COMPOUND

On the basis of previous work in this laboratory, the selection of an appropriate potting compound was focused on a single series of formulations. These consist of a 100-percent-reactive epoxy resin adhesive and an activator. The system requires a 2-h cure at 165°F (74°C). The two components may be combined in different resin/activator ratios to provide different mechanical properties. The designations and some of the properties for several mixture ratios are given in Table 1.

TABLE 1

MECHANICAL PROPERTIES OF CW-SERIES POTTING COMPOUNDS

	Resin/activator ratio			
	2:3	1:1	3:2	2:1
Designation	C2W3	C1W1	C3W2	C2W1
Bond strength [(a)],				
lbf/in^2	2450	3280	-	-
(MPa)	(16.9)	(22.6)	-	-
Compressive strength [(a)],				
lbf/in^2	32200	20700	-	-
(MPa)	(222)	(143)	-	-
Elongation [(a)], percent	8.0	7.0	-	-
Elastic modulus [(b)],				
lbf/in^2	51000	275000	316000	-
(GPa)	(0.35)	(1.90)	(2.18)	-

(a) According to the manufacturer.

(b) From compressive tests on 0.5-in (13-mm) diameter specimens performed in this laboratory.

A simple, shear-type end fitting was fabricated to evaluate the relative pullout shear strengths of the several CW potting compounds. This fitting consists of a cylindrical metal sleeve which is attached to an FRP rod with a thick layer of potting compound.

A series of twelve tensile tests was performed using 1/2-in (13-mm) diameter, high-strength FRP rod. All twelve specimens failed by rod pullout and the results are given in Table 2. Although there is great scatter in these data, the relatively high strengths of the specimens with the most flexible potting compound are significant. These results support the analytical parameter study which showed that a more flexible potting compound produces significantly lower peak bond-shear stresses. Finite-element analyses of the fitting indicate that the peak bond-shear stress with the most flexible C2W3 potting compound is only 47 percent of the corresponding stress with the stiff C3W2 compound.

3. DEVELOPMENT OF THE MOD 4 END FITTING

The Mod 4 end fitting, Figure 5, is a shear-type potted end fitting which relies upon its long length to achieve high shear strength at the interface between the rod and the potting compound. To mount the fitting on an FRP rod, the end of the rod, after abrasive cleaning, is set into the hole at the base of the cavity. The rod is carefully

TABLE 2

PULLOUT TESTS OF CW-SERIES POTTING COMPOUNDS

Test No.	Potting compound	Maximum load lbf	Maximum load (kN)
71169	C2W3	19850	88.3
71170	C2W3	15500	68.9
71171	C2W3	18650	83.0
Average		18000	80.1
71166	C1W1	12200	54.3
71167	C1W1	8500	37.8
71168	C1W1	19250	85.6
Average		13300	59.2
71172	C3W2	8000	35.6
71173	C3W2	14350	63.8
71174	C3W2	9400	41.8
Average		10600	47.1
71175	C2W1	12350	54.9
71176	C2W1	17500	77.8
71177	C2W1	18100	80.5
Average		16000	71.2

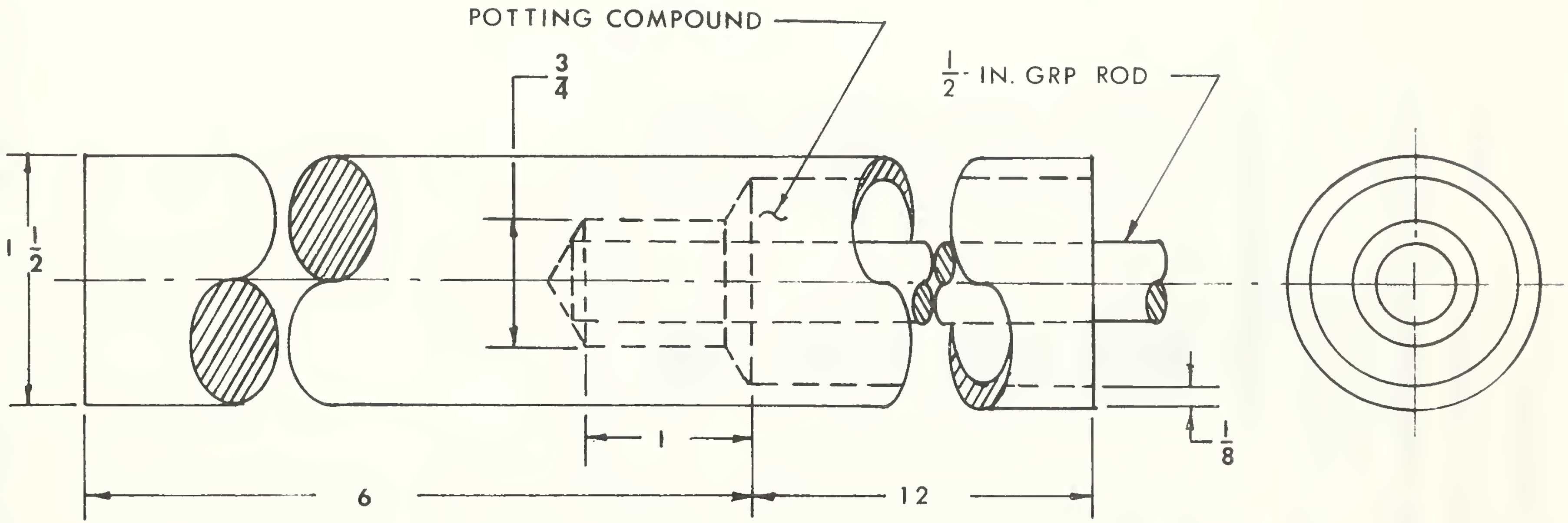

Figure 5 - NBS Mod 4 Experimental End Fitting for 1/2-in (13-mm) Diameter Rod. All Dimensions in Inches (1 in = 25.4 mm).

alined parallel and concentric with the fitting and the remaining cavity is filled with the potting compound. The fitting was designed primarily for 1/2-in (13 mm) diameter rod, which leaves a 3/8-in (10-mm) thickness of potting compound around the rod.

A tensile specimen was fabricated by mounting two Mod 4 end fittings on a length of 1/2-in (13-mm) diameter FRP rod using the C2W3 potting compound. The specimen was instrumented with twenty-six resistance strain gages for experimental stress analyses under tensile loading. The results of these measurements [5, 14] suggest that under high loads the bond-shear stress on the surface of the rod is roughly uniform over most of the potted length. This uniformity is believed to be a major factor contributing to the relatively high strength of the Mod 4 end fitting which was subsequently observed with tensile specimens that had been potted with the flexible C2W3 compound.

The performance of the Mod 4 end fitting was evaluated by means of tensile tests on two commercially available FRP rod materials of 1/2-in (13-mm) diameter. Both are fabricated from unidirectional, continuous, E-glass roving and a polyester resin matrix. The manufacturing process for one of these materials, Material E, results in the formation of an integral gel coating of the matrix material on the outer surface of the rod. The second material, Material N, is coated with a filled epoxy for resistance to weathering.

The results of twenty tensile tests using Mod 4 fittings on Materials E and N rods are given in Table 3. The low-modulus C2W3 potting compound was used on all specimens. Two of the seventeen Material E specimens

TABLE 3

TENSILE TESTS WITH MOD 4 END FITTINGS ON 1/2-IN (13-mm) FRP ROD. POTTING COMPOUND: C2W3

Test No.	Material	Maximum load lbf	(kN)	Failure
71182	E	31350	(139)	(a)
71183	E	32850	(146)	(b)
71184	E	25750	(115)	(a)
81242	E	27000	(120)	(a)
81243	E	28600	(127)	(a)
81244	E	32600	(145)	(a)
81245	E	29600	(132)	(a)
81246	E	29000	(129)	(a)
81247	E	31800	(141)	(a)
81248	E	32750	(146)	(a)
81249	E	30950	(138)	(a)
81250	E	31100	(138)	(a)
81251	E	31500	(140)	(a)
91261	E	23250	(103)	(c)
101315	E	30100	(134)	(a)
101333	E	31850	(142)	(a)
101404	E	31500	(140)	(b)
Average:		30100	(134)	
81240	N	23700	(105)	(a)
81241	N	17850	(79)	(a)
91263	N	18900	(84)	(a)
		20150	(90)	

(a) Pullout.

(b) Failure in the free length.

(c) Pullout; potting compound did not appear to have been adequately cured.

failed in the free length at loads of 32850 and 31500 lbf (146 and 140 kN). The other fifteen Material E specimens failed by pullout with the failure located principally at the interface between the rod and the potting compound. The average maximum load for all of the Material E specimens was 30100 lbf (134 kN), which is more than 90 percent of the loads attained by the specimens which failed in their free lengths. This indicates that the full tensile strength of Material E is approached with the Mod 4 fittings.

The average maximum load for three specimens of Material N with Mod 4 end fittings was only 20150 lbf (90 kN). Failure here was also by pullout but in this case the failure was within the rods with several of the outer layers of glass fibers being sheared off.

A comparison of these results with those obtained with commercial end fittings [5] reveals that the Mod 4 end fitting is clearly superior to the commercial types for Material E. For Material N the performance of the Mod 4 fitting is equal to that of the commercial types although it does not, apparently, allow the full tensile strength of Material N to be approached.

Several modifications were explored in an attempt to improve the performance of the Mod 4 end fitting on Material N. These modifications involved (1) increasing the size of the fitting, (2) using potting compounds with formulations different from those of the CW series, and (3) driving wedges into the ends of the rods prior to potting. The results of these studies [16] showed no improvement over those obtained with the standard Mod 4 end fitting.

Some numerical experiments were conducted on the computer in an effort to obtain a greater understanding of the process of load transfer from the end fitting, through the potting compound, to the rod. This effort indicated the feasibility of incorporating the nonlinear properties of polymeric potting compounds into the finite-element analysis. This type of nonlinear analysis has been used in this laboratory to study composite-reinforced cutouts in metal sheet [17]. However, it was determined that this approach could not be effectively pursued within the resources available on the present program.

4. DEVELOPMENT OF THE H3M END FITTING

Since the Mod 4 end fitting was found to be incapable of developing the full tensile strength of Material N, it was decided to investigate the performance of compression-type, rather than shear-type, end fittings for this material. Accordingly, a series of tension tests was performed using two different compression-type potted end fittings. One of these is a commercially available fitting and the other was developed in this laboratory in an earlier program.

The Type R/P end fitting, Figure 6, is a commercially available, basket type, potted, compression fitting which is intended primarily for synthetic ropes. The conical basket, or potting head, is fitted with a yoke and bail for attachment to thimble-eye type hardware. To mount the Type R/P fitting on an FRP rod, a fluted, cruciform wedge (Fig. 7) was first driven axially into the end of the rod. (These metal wedges are available from the manufacturer of Material N). The inner surface of the potting head is treated with an epoxy-release agent, then the rod is alined parallel and concentric with the fitting, which is

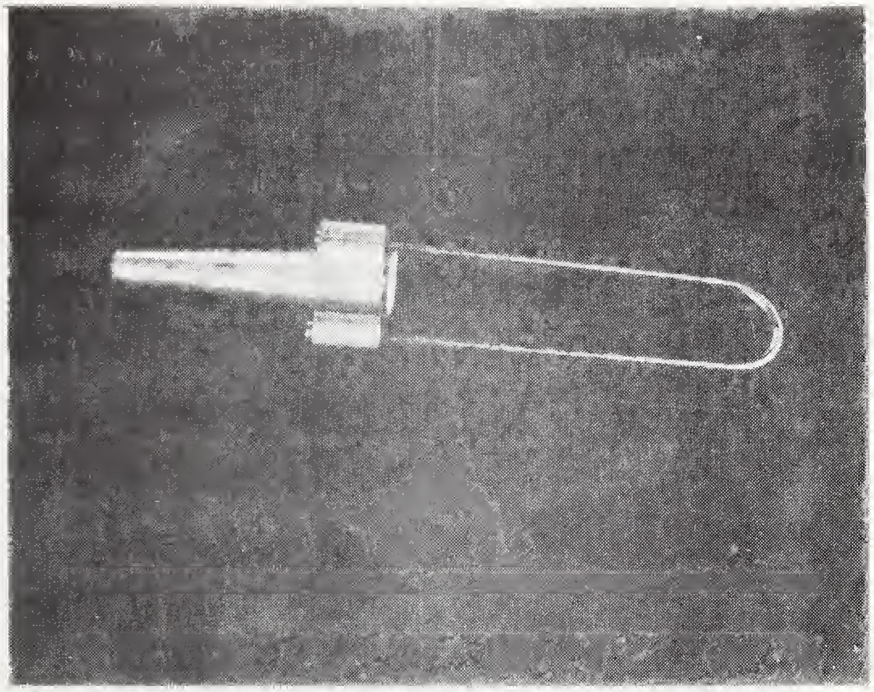

Figure 6 - Commercially Available Type R/P End Fitting for 1/2-in (13-mm) Diameter Rope

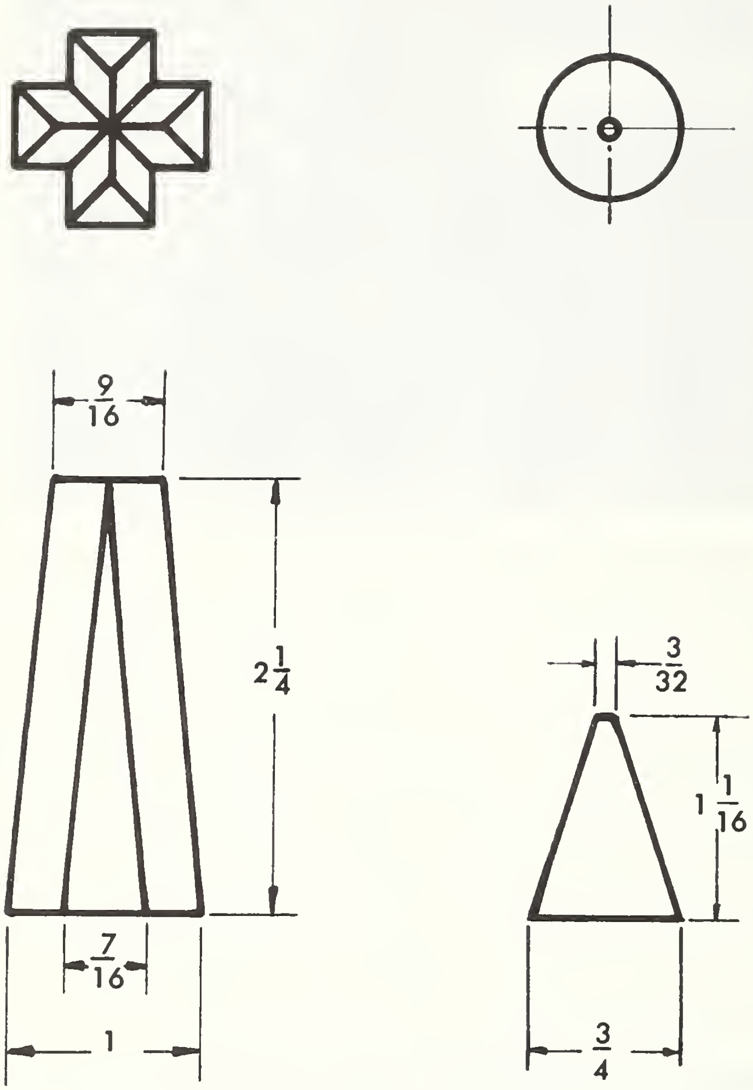

Figure 7 - Cruciform (left) and Conical (right) Wedges for 1/2-in (13-mm) Diameter Rod. All Dimensions in Inches (1 in = 25.4 mm)

then potted and cured. The release agent permits the potted material to slide relative to the potting head, and under tensile loads the potted end seats tightly into the conical potting head. This seating process develops significant radial compressive stresses in the potted end which enhance the strength of the bond between the rod and the potting compound. The release agent also facilitates removal of the potted material for reuse of the fitting.

The NBS aluminum-block end fittings, Figure 8, were developed in an earlier investigation [13]. The wedging and potting procedures for these fittings are the same as those described above the Type R/P end fittings.

These two types of fittings were used in a series of eight tensile tests on Material N in an earlier study [13]. For those tests conical wedges (Fig. 7) and C1W1 potting compound (Table 1) were used. Except for one test in which the rod pulled out of the fitting prematurely, all of the specimens failed at loads between 20500 and 22300 lbf (91 and 99 kN) by pinching off at the fitting due to the radial compressive stresses.

Four additional tensile tests of Material N were performed in the present investigation using these two types of end fittings. In these tests the cruciform wedges were used. The C2W3 potting compound was used for two of the specimens on the basis of the analytical parameter study. PC8 potting compound* was selected for the other two specimens because of its high compressive strength. The results of the tests are given in Table 4. These results show that the aluminum-block end fitting

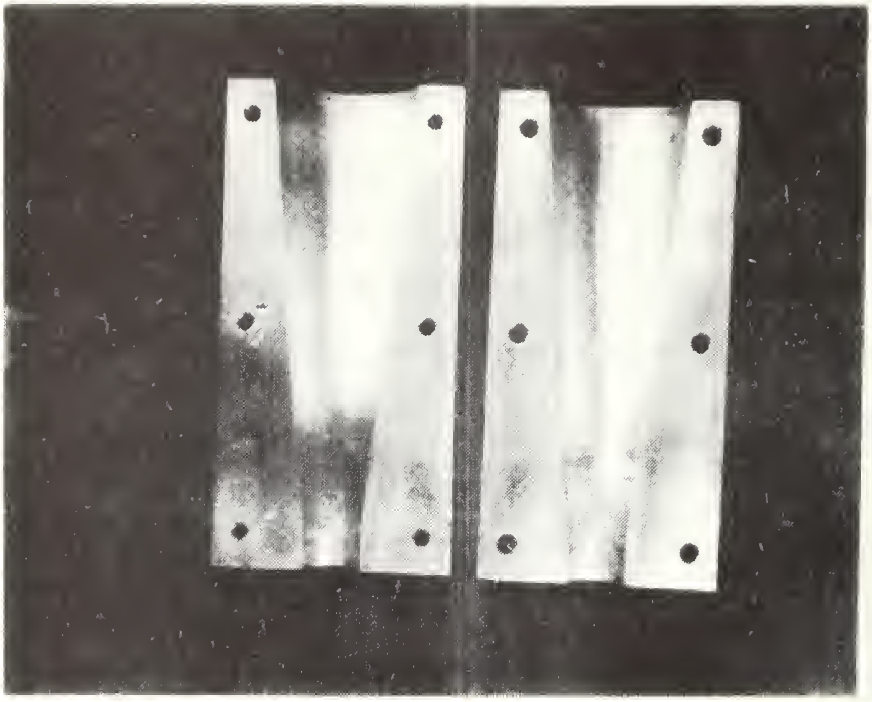

Figure 8 - NBS Aluminum-Block Experimental End Fitting for 1/2-in (13-mm) Diameter Rod

TABLE 4

TENSILE TESTS OF 1/2-IN (13-mm) MATERIAL N WITH COMPRESSION-TYPE POTTED END FITTINGS.

Test No.	End fitting	Potting compound	Maximum load		Failure
			lbf	(kN)	
101408	R/P	PC8	21950	(98)	(a)
101410	R/P	C2W3	21000	(93)	(a)
101409	Al-block	PC8	24350	(108)	(b)
101411	Al-block	C2W3	26050	(116)	(b)

(a) Initiated in the end fitting.

(b) In the free length.

is capable of developing the full tensile strength of Material N rod and verified the superiority of the C2W3 potting compound. The maximum load in Test No. 101411 is the highest ever achieved in this laboratory on 1/2-in (13-mm) Material N at room temperature.

The aluminum-block end fitting was subsequently redesigned [16] in a cylindrical, one-piece configuration, and assigned the laboratory designation H3M. See Figure 9. These changes were made in order to reduce the cost of the fitting and to facilitate its use in the testing machine which was employed for the tensile tests in this investigation. The changes have no major effect on the performance of the fitting.

Two more tensile tests were performed to examine the relative performances of the conical wedge and the fluted, cruciform wedge when used with the H3M end fitting. For these tests Material E rod and C2W3 potting compound were employed. The specimen with the cruciform wedges failed in its free length at 33450 lbf (14 kN). This is the highest breaking load ever achieved in this laboratory on 1/2-in (13 mm) Material E rod. The specimen with the conical wedges pulled out of the end fitting at 32900 lbf (146 kN). On the basis of these results it was decided to continue using the cruciform wedges, which are available commercially at less cost than the conical wedges, which had been manufactured in-house.

---

*PC8 is a two-component, 100-percent solids, liquid epoxy pouring compound having a prescribed mixing ratio.

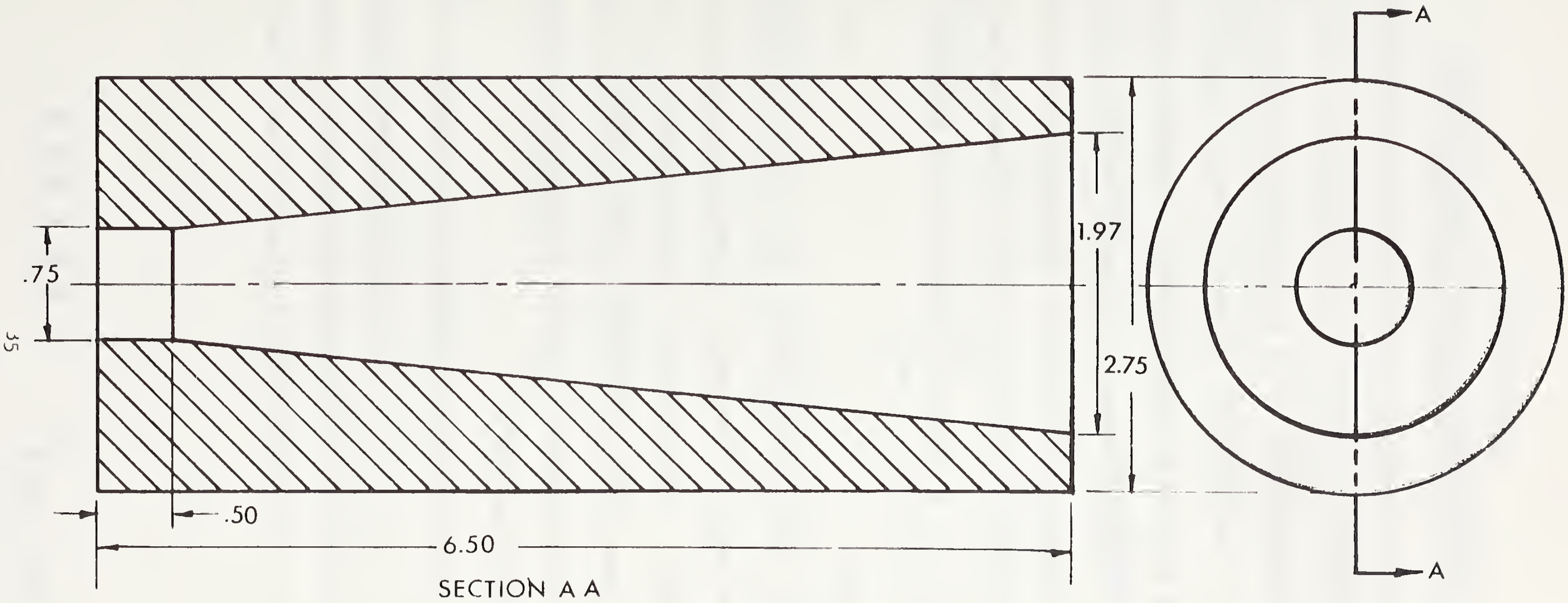

Figure 9 - NBS H3M Experimental End Fitting for 1/2-in (13-mm) Diameter Rod. All Dimensions in Inches (1 in = 25.4 mm)

SECTION V

PARAMETER STUDY OF THE MANUFACTURING PROCESS, PART I

During this part of the effort toward optimizing the manufacturing process for pultruded FRP rod, eleven different samples of 1/2-in (13-mm) diameter rod were manufactured using E-glass roving (Table 5) and an isophthalic polyester resin matrix (Table 6). These samples were designed to examine the effects of nine different process parameters using two values, or settings, of each parameter. On the basis of the pultruder's experience, plus the results obtained from a preliminary sample which had been manufactured and tested previously [16], constant values were assigned to three additional process parameters for the purposes of this study.

1. PROCESS PARAMETERS

a. Roving Preheat. Earlier studies had shown that the wetting of the fibers by the resin might be improved by preheating the rovings to drive off surface moisture. This was done, in this program, by passing the rovings through an oven prior to their entry into the dip trough. The oven is 54 in (1.4 m) long and is capable of continuous operation between 250 and 300°F (120 and 150°C).

b. Roving Twist. Glass roving is commercially available either twisted or untwisted. The use of untwisted roving could conceivably facilitate wetting and might also be conducive the achieving straight, parallel fibers in the finished product. On the other hand, since twisted rovings have

TABLE 5

CHARACTERISTICS OF GLASS FIBER ROVING[a]

Type:	E-glass (electrical grade), continuous
Fiber diameter:	K (0.00052 in, 13 um, nominal)
Fibers per strand:	400, nominal
Roving yield:	

End count[b]	Nominal yield yd/lb	(m/kg)
30	123 ± 6	(301 ± 15)
60	61.5 ± 3.1	(151 ± 8)

Specific gravity[c]:	2.45
Type of binder:	Silane (proprietary formulation)
Percent of binder:	0.55 ± 0.15, by weight (mass) of glass
Tensile strength[d]:	>200,000 lbf/in^2 (>1400 MPa)

(a) According to the manufacturer, except as noted.

(b) Number of strands per roving.

(c) Calculated.

(d) Per ASTM Designation D-2343 [18].

TABLE 6

CHARACTERISTICS OF ISOPHTHALIC POLYESTER RESIN [(a)]

Monomer:	Styrene, approximately 30 percent.
Viscosity:	23-27 poise at 77°F (2.3-2.7 Pa·s at 25°C)
Specific gravity:	1.12 - 1.13 at 77°F (25°C)
Reactivity:	Medium
Cure data[(b)]:	
Gel time:	3-4 minutes.
Time to peak:	4.5 - 5.5 minutes.
Peak temperature:	390 - 410°F (200 - 210°C)

(a) According to the manufacturer, for matched-metal-die molding applications.

(b) Per SPI procedure [19].

less fuzz and catenary, these might, in fact, result in better collimated fibers. Both twisted and untwisted rovings were used.

c. Roving End Count. Glass roving is also available in a wide range of end counts (number of strands per roving). The pultrusion of a larger number of rovings with a smaller end count could, perhaps, provide a more uniform distribution of fibers throughout the cross section. At the same time, the difficulties in achieving good collimation probably increase with the number of rovings used. End counts of 30 to 60 were examined.

d. Roving Tension. It had been observed that the fibers in pultruded rod are frequently not straight. In the present work, therefore, several samples were manufactured with the fibers pretensioned to straighten them. This was accomplished by passing the rovings over an S-bend, as shown in Figure 10. Initially, the vertical separation of the two rods which form the S-bend was 6 in (150 mm) and the horizontal separation was 4 in (100 mm). Later, to increase the tension, the vertical separation was reduced to 3 in (80 mm) and the horizontal separation increased to 5 in (130 mm). In addition, each roving was passed through an eyebolt, as shown in the figure. The individual eyebolts were rotated, as necessary, to approximately equalize the tension in the various rovings.

e. Roving Collimation. In addition to being straight it is also important that the rovings be alined parallel to the axis of the rod. This was promoted by constraining the rovings to follow essentially parallel paths through the dip trough. The rovings were passed through a series

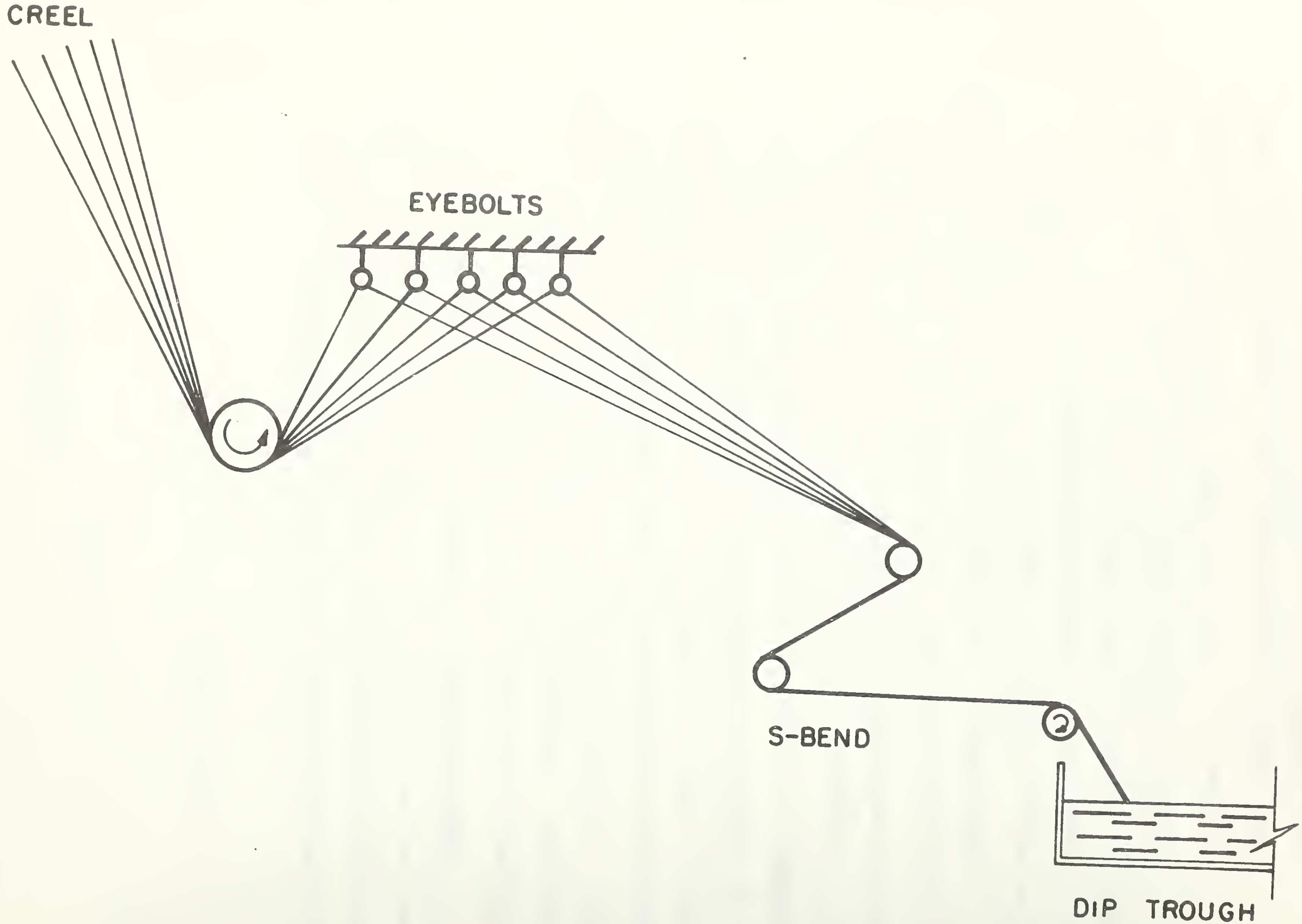

Figure 10 - Schematic Representation of Tensioning Apparatus for Pultrusion

of three polyethylene guide plates which were mounted in the dip trough, Figure 11. Each plate contained holes -- one hole for each roving -- arranged in a pattern of concentric circles. All of the holes were below the resin level in the trough, and the middle guide plate was set somewhat higher than the other two to introduce some tension into the rovings. After passing through the third guide plate the rovings followed an essentially horizontal path to the die, leaving the dip trough through a 5/8-in (16-mm) orifice beneath the surface of the resin.

This apparatus is believed to reduce the inadvertent intertwining of rovings, and to promote resin penetration by separating the mass of rovings in the trough.

f. Immersion Length. The wetting of the fibers with the resin could conceivably be improved by increasing the duration of the immersion in the dip trough. This can be accomplished either by reducing the pulling speed of the rovings or by increasing the immersion length in the dip trough. In this program pulling speed was maintained constant, as discussed below, and the effects of immersion time were examined by using either a "standard" dip trough, which provides an immersion length of approximately 23 in (0.6 m), or a long trough, for an immersion length of approximately 54 in (1.4 m).

g. Ultrasonic Agitation. Another approach to improving fiber wet-out involves the use of ultrasonic excitation to agitate the fibers and drive entrapped air from the rovings. In this program a 250-W ultrasonic exciter, which vibrates at 20000 Hz, was used in the manufacturing process

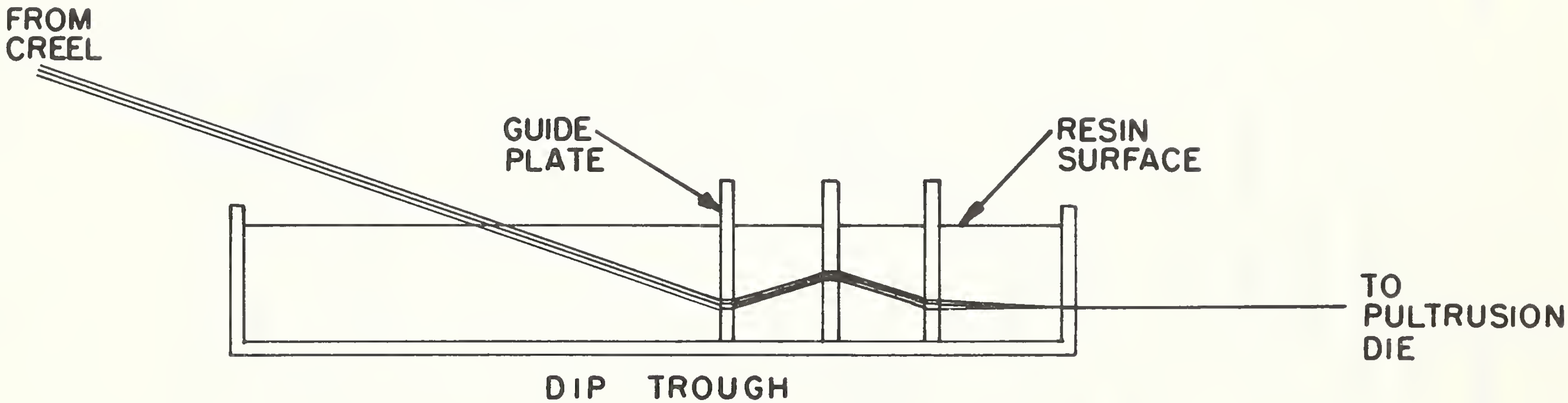

Figure 11 - Schematic Representation of Collimating Apparatus for Pultrusion

for several samples. It was found that the ultrasonic vibrations were damped out, and the instrument rendered inoperative, when the end of the ultrasonic horn was immersed in the dip trough to a depth exceeding about 1/16 in (2 mm). Therefore, the end of the horn was placed in contact with the rovings near the point of their emergence from the resin.

h. Wetting Agent. Improved wetting of the fibers was also sought through the use of a wetting additive in the resin system. Polycaprolactone [20] was selected for this purpose on the basis of its demonstrated ability to facilitate the dispersion of glass particles in resins [21]. It is commercially available in flake form and, according to the manufacturer, is readily compatible with styrene-unsaturated polyesters. In low concentrations it also imparts improved surface properties to glass-reinforced plastics [22].

i. Resin System Formulation. On the basis of prior experience it was known that the resin system should have a dynamic viscosity in the range of 11.5 to 13.0 poise (1.15 to 1.30 Pa·s) for satisfactory pultrusion. This was accomplished by adding monostyrene to the isophthalic polyester resin. The proportion of monostyrene had to be increased when the polycaprolactone wetting agent was used since the latter tends to raise the viscosity of the system. The resin system formulation, both with and without the wetting agent, is given in Table 7.

j. Curing Conditions. With a given resin system and a given length of heated die, attainment of a satisfactory cure primarily depends upon two parameters: the pulling speed and the die temperature.

95

TABLE 7

RESIN SYSTEM FORMULATION, RUNS 1 - 11

	Without wetting agent wt (mass) pct	With wetting agent wt (mass) pct
Monostyrene	4.91	7.09
Peroxide catalyst	0.73	0.70
Die lubricant	0.92	0.86
Ultraviolet inhibitor	0.13	0.12
Wetting agent	-	4.96
Isophthalic polyester resin	Bal.	Bal.

From the results on a preliminary sample [16] a pulling speed of 12 in/min (5 mm/sec) and a thermostat setting of 350°F (177°C) on the curing die were selected. These two processing parameters were maintained for all of the pultrusion runs.

k. Post Curing. At normal pultruding speeds each increment of rod is exposed to the curing die for a very short time and it is not possible to effect a complete cure in this interval. Although cure undoubtedly proceeds to completion under ambient conditions over a period of months, the addition of a post cure to the manufacturing process would provide the benefits of a complete cure from the outset. These benefits may include enhanced weather resistance as well as increased strength. This parameter was examined by adding a post cure of 16h at 275°F (135°C) to the manufacturing process for one sample.

2. DESIGN OF EXPERIMENT

Nine of the variable process parameters were examined in two values, or settings, of each. For example, the effects of roving end count were investigated by manufacturing some rod samples with 30-end roving and others with 6-end roving. For most of the parameters, however, the two values, or settings, consisted of a "yes" or "on" condition and a "no" or "off" condition. Thus, the effects of ultrasonic agitation were investigated by manufacturing some rod samples with agitation (the "yes" setting) and others without agitation (the "no" setting). The nine parameters and their settings were:

Roving preheat (yes, no)
Roving twist (yes, no)
Roving end count (60, 30)
Roving tension (yes, no)
Roving collimation (yes, no)
Immersion length (long, standard)
Ultrasonic agitation (yes, no)
Wetting agent (yes, no)
Post curing (yes, no).

Three other process parameters (resin viscosity, pulling speed, die temperature) were kept constant.

Eleven samples of rod were manufactured. Table 8 gives the selected settings of the nine variable process parameters for each of Runs 1 through 11. This scheme permits the effects of each of three parameters (preheat, collimation, post curing) to be examined by comparing the properties of two samples, which had been manufactured such that all of the process parameters were the same for both except the parameter being studied. Thus, for example, the process parameters for Runs 1 and 2 were nominally identical except that the roving was preheated in Run 2 while in Run 1 it was not.

The remaining six variable parameters (twist, end count, tension, immersion length, ultrasonics, wetting agent) were investigated more extensively using eight rod samples. The parameter settings for these eight manufacturing runs were designed by Dr. G. M. Jouris of the Mathematics Department at the Westinghouse Research Laboratories such that each of the six variable parameters occurs four times at its high or "yes" setting and four times at its low or "no" setting. The other three variable parameters (preheat, collimation, post curing) were kept constant throughout these eight manufacturing runs. This method permits samples from all eight runs

TABLE 8

SELECTED SETTINGS OF THE VARIABLE PROCESS PARAMETERS FOR MANUFACTURING RUNS 1 THROUGH 11

Run No.	Roving preheat	Roving twist	Roving end count	Roving tension	Wet-ting agent	Immer-sion length	Ultra-sonic agita-tion	Colli-mation	Post cure
1	No	Yes	60	No	No	Std	No	No	No
2	Yes	Yes	60	No	No	Std	No	No	No
3	Yes	Yes	60	No	Yes	Long	Yes	No	No
4	Yes	Yes	30	Yes	Yes	Std	No	No	No
5	Yes	Yes	30	Yes	No	Long	Yes	No	No
6	Yes	No	60	Yes	No	Long	No	No	No
7	Yes	No	60	Yes	Yes	Std	Yes	No	No
8	Yes	No	30	No	Yes	Long	No	No	No
9	Yes	No	30	No	No	Std	Yes	No	No
10	Yes	Yes	60	No	No	Std	No	Yes	No
11	Yes	Yes	60	No	No	Std	No	No	Yes

to be used in making a decision about each of the six variable parameters being studied. A large difference between the average value of a given rod property at the high setting, and the average value of that property at the low setting, indicates that the property is sensitive to the variable parameter. Conversely, a negligible difference suggests that the property is essentially independent of the variable parameter.

Examination of Table 8 shows which samples must be compared in order to evaluate the effects of each variable process parameter. This information is summarized in Table 9. This table shows, for example, that in order to evaluate the effect of twist in the roving, the average properties of the rods from Runs 2, 3, 4 and 5 (which contain twisted roving) should be compared with the average properties of the rods from Runs 6, 7, 8 and 9 (which contain untwisted roving).

3. MANUFACTURE OF EXPERIMENTAL MATERIALS

Eleven samples of 1/2-in (13-mm) diameter glass-reinforced-polyester rod were manufactured in accordance with the process parameter settings given in Table 8. Some of the operating conditions for these manufacturing runs are given in Table 10 and discussed below.

a. Number of Rovings. The number of rovings used in the manufacture of each sample was not arbitrary but was determined by the amount of glass needed to produce good quality rod under the preselected processing conditions. The use of tension, for example, made it necessary to increase the number of rovings to properly fill out the die. The glass contents in the finished samples were measured by the manufacturer and are reported

TABLE 9

EVALUATION OF THE VARIABLE PROCESS PARAMETERS

To evaluate the effect of:	Compare the average rod properties from these runs (high or "yes" setting)	with (low or "no" setting)
Preheat	2	1
Collimation	10	2
Post Cure	11	2
Twist	2, 3, 4, 5	6, 7, 8, 9
End Count	2, 3, 6, 7	4, 5, 8, 9
Tension	4, 5, 6, 7	2, 3, 8, 9
Immersion Length	3, 5, 6, 8	2, 4, 7, 9
Ultrasonics	3, 5, 7, 9	2, 4, 6, 8
Wetting Agent	3, 4, 7, 8	2, 5, 6, 9

TABLE 10

OPERATING CONDITIONS FOR MANUFACTURE OF RUNS 1 THROUGH 11

Run No.	No. of rovings	Glass content	Ambient relative humidity	Ultrasonic loading	S-bend spacing (a)		Resin temperature	
		wt (mass) pct	percent	W	in	(mm)	°F	(°C)
1	22	70.8	30-31	-	-	-	(b)	(b)
2	22	70.7	30-31	-	-	-	(b)	(b)
3	22	71.9	36-38	200-225	-	-	82-100	(28-38)
4	46	73.8	16-18	-	4,6	(100,150)	81-86	(27-30)
5	49	76.2	20-23	238-250	4,6	(100,150)	84-93	(29-34)
6	23	73.4	22-25	-	5,3	(130,80)	74-79	(23-26)
7	23	73.8	18-21	250	5,3	(130,80)	108-118	(42-48)
8	44	71.9	24	-	-	-	77-81	(25-27)
9	44	70.6	22-25	150-175	-	-	68-106	(20-41)
10	23	73.7	25	-	-	-	(b)	(b)
11	22	70.7	27-28	-	-	-	(b)	(b)

(a) x,y means x inches (mm) horizontal spacing, y inches (mm) vertical spacing.

(b) Not measured, approximately ambient.

in Table 10. Note that for a given glass content twice as many 30-end rovings are required as 6-end rovings.

b. Ultrasonic Loading. The ultrasonic generator was operated at the minimum power level required to maintain loading of the ultrasonic horn without stalling. When tension was used on the glass roving, increased power was required to keep the horn operating.

c. Resin Temperature. Use of ultrasonic agitation caused the temperature of the resin in the dip trough to rise, resulting in partial polymerization of the resin. This problem was serious when the standard immersion length was used rather than the long immersion length since, in the latter case, the energy could be dissipated to a greater volume of resin. In Run 9, for example, which employed the standard immersion length, the increased resin temperature made it necessary to remove 2- to 3-oz (60- to 90-g) chunks of gelled resin, from the vicinity of the horn, at 15- to 20-min intervals. Small resin additions were, therefore, frequently required in order to maintain the proper resin level, and this helped to control the temperature rise.

The higher power levels required for ultrasonic agitation, when roving tension was used, increased the heating problem. In Run 7, when ultrasonic agitation was used in conjuction with roving tension and a standard immersion length, the problem became most severe and the dip trough had to be cooled externally. This was only partially successful, and it was necessary to discontinue this run after only about 60 ft (20 m) of rod had been pultruded.

A certain amount of resin heating was found to be desirable when the wetting agent was used since it tended to separate from the resin solution at temperatures below about 77°F (25°C). Consequently, infrared lamps mounted beneath the dip trough were employed when ultrasonic agitation was not being used.

4. TESTS AND RESULTS

The more important properties of the rods, from Runs 1 through 11, were evaluated by means of the test methods and measurement techniques described earlier. The average results of some of these tests and measurements are given in Table 11.

a. Tensile Breaking Load. The tensile tests of rod specimens from Runs 1 through 11 were performed at room temperature. Forty-one tests were carried out at a crosshead speed of 0.75 in/min (0.32 mm/s) and nineteen at 300 in/min (130 mm/s). The results of these tests are given in the Appendix; they are summarized in Table 12. Failure in all but two of the high-speed tensile tests initiated in an end fitting. Such results indicate that the breaking load of the rod was greater than that corresponding to the maximum load.

b. Stress-Rupture Tests. Eighty-three stress-rupture tests were carried out on rod specimens from Runs 1 through 11 under saturated humidity conditions. Thirty-eight of these tests were performed at 160°F (71°C) and forty-five at 200°F (93°C). The original intent of the tests was to study the stress-rupture strength of each sample of material, at each temperature, over the time range from 1 to 1000 h. It was soon realized,

TABLE 11

AVERAGE DIMENSIONS AND PHYSICAL PROPERTIES, RUNS 1 - 11

Run No.	Diameter		Density		Weight	(mass)	Rockwell hardness (Scale E)	Transverse tensile strength		Wet breakdown voltage
	in	(mm)	lb/in^3	(Mg/m^3)	lb/ft	(kg/m)		lbf/in^2	(MPa)	kV
1	0.501	(12.7)	0.0690	(1.91)	0.164	(0.244)	53	1300	(9)	22
2	.502	(12.8)	.0691	(1.91)	.164	(.244)	51	1300	(9)	22
3	.496	(12.6)	.0695	(1.92)	.161	(.240)	24	2200	(15)	43
4	.496	(12.6)	.0708	(1.96)	.164	(.244)	34	1400	(10)	23
5	.497	(12.6)	.0722	(2.00)	.168	(.250)	53	1600	(11)	29
6	.496	(12.6)	.0712	(1.97)	.165	(.246)	56	1700	(12)	25
7	.495	(12.6)	.0711	(1.97)	.164	(.244)	44	1900	(13)	35
8	.495	(12.6)	.0698	(1.93)	.161	(.240)	42	2000	(14)	45
9	.485	(12.3)	.0697	(1.93)	.161	(.240)	47	1200	(8)	19
10	.496	(12.6)	.0708	(1.96)	.164	(.244)	47	1200	(8)	20
11	.501	(12.7)	.0692	(1.92)	.164	(.244)	62	1800	(12)	22

TABLE 12

AVERAGE TENSILE BREAKING LOADS, RUNS 1 - 11

Run No.	Average breaking load			
	Conventional		High-speed	
	lbf	(kN)	lbf	(kN)
1	29000	(129)	36000	(160)
2	29100	(129)	>34700	(>154)
3	27100	(121)	>37000	(>165)
4	22500	(100)	>29000	(>129)
5	23000	(102)	>32500	(>145)
6	24700	(110)	38100	(169)
7	26200	(117)	(a)	(a)
8	25900	(115)	>34000	(>151)
9	28000	(125)	>36000	(>160)
10	30400	(135)	>34000	(>151)
11	29600	(132)	>32500	(>145)

(a) Not tested.

however, due to scatter in the test results and to the occasional occurrence of failures which initiated in the end fittings, that far more tests would be required to characterize the stress-rupture strengths than had been planned. Some trade-offs were effected by conducting fewer tests on samples which exhibited low stress-rupture strengths so that additional tests could be conducted on the other samples. In particular, no tests were carried out at loads less than 10000 lbf (44 kN) because 1/2-in (13-mm) rods with stress-rupture capacities below this are clearly not competitive with commercially available products.

The results of the stress-rupture tests are given in the Appendix. These results show several interesting features. If the data are plotted on semi-log coordinates (see, for example, Fig. 12) the slope of the curve of load vs log time-to-rupture becomes increasingly negative with increasing time. This is contrary to the behavior of most stress-rupture data. Also, there was no clear distinction between the stress-rupture properties at 160°F (71°C) and those at 200°F (93°C). Certain samples of material appeared to be stronger at the higher temperature, particularly at longer rupture times (see, for example, Fig. 13).

An explanation of this seemingly anomalous behavior is given in Section V.4.C in terms of identifiable, opposing damage mechanisms. The existence of the negative temperature effect ruled out the straightforward use of reaction-rate analysis techniques to characterize the stress-rupture properties of the various samples. In fact, the existence of the unusual temperature and time effects made it difficult to even rank the eleven samples in terms of their stress-rupture strengths. It was recognized,

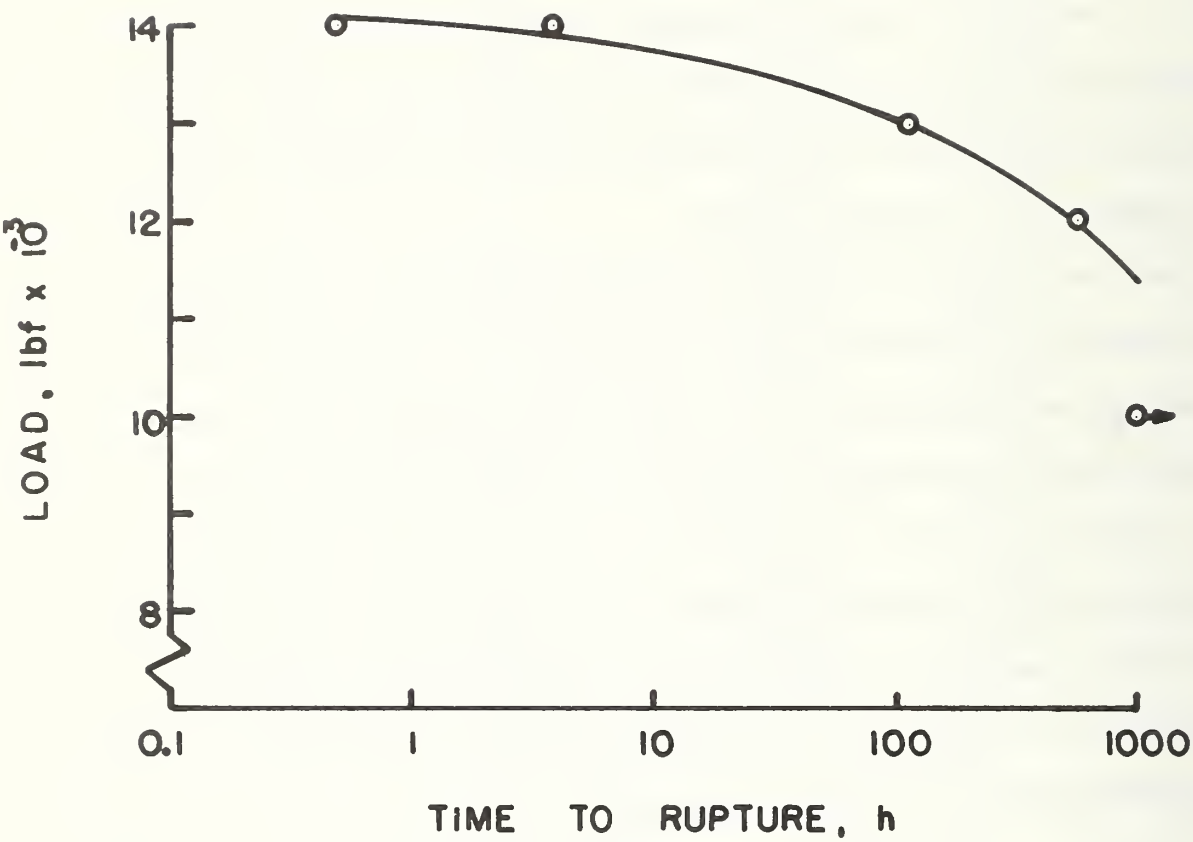

Figure 12 - Stress-Rupture Properties of Rod from Run 1 at 200°F (93°C) under Saturated Humidity. (1 lbf = 4.45 N.)

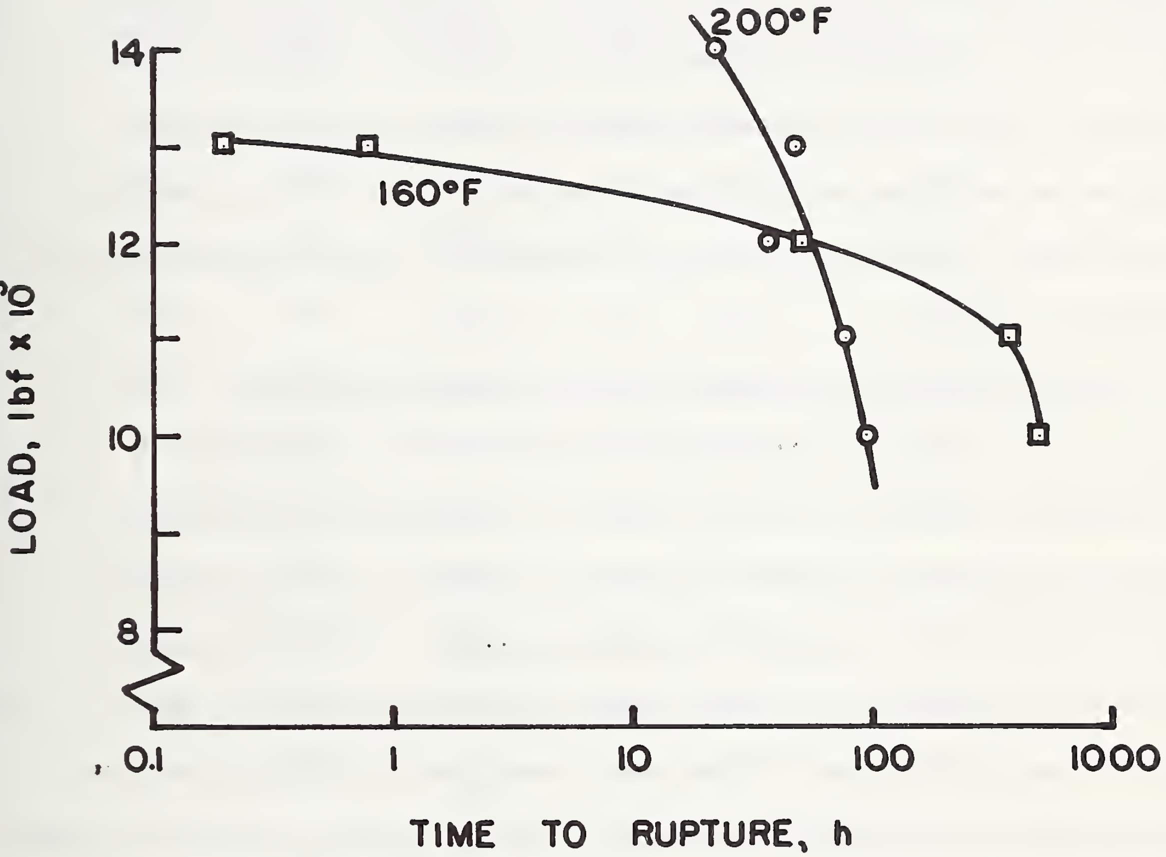

Figure 13 - Stress-Rupture Properties of Rod from Run 2 at 160 and 200^{o}F (71 and 93^{o}C) under Saturated Humidity. (1 lbf = 4.45 N.)

however, that a ranking would be very helpful in assessing the effects of the various processing parameters. Accordingly, the 100-h stress-rupture load was arbitrarily selected as the characteristic which would be used for comparing the anticipated weatherabilities of the samples. Values of the 100-h stress-rupture loads were derived by interpolating -- and, in some cases, extrapolating -- the test data. In so doing, considerable judgement had to be exercised regarding the shapes of the rupture curves between data points. The derived values are given in Table 13 and must be regarded as estimates at best; the table is provided solely to enable the most general comparisons to be made between the stress-rupture strengths of different samples.

c. Mechanism of Stress-Rupture under Hot, Humid Conditions. An explanation of the unusual stress-rupture behavior which was observed in the pultruded rod samples may be obtained by considering the effects of the moisture-laden environment. Before the moisture can affect the properties of the rod, it must pass through two stages. First, the water vapor in the saturated-humidity environment must be adsorbed onto the surface of the rod specimen. The moisture must then diffuse from the adsorbed film into the interior of the rod. Since diffusion is a time-dependent process it might be expected that for short periods of test time (i.e., high test loads) the stress-rupture properties would be essentially unaffected by the humid atmosphere. As time increases, more and more moisture is diffused further into the interior of the rod. Then the detrimental effects of water on the elevated-temperature strength of glass-fiber composites [23, 24] produce the increasingly negative slope of the rupture

TABLE 13

ESTIMATED STRESS-RUPTURE LOADS, RUNS 1 - 11

Run No.	Tensile load to produce rupture in 100h at					
	160°F	(71°C)	200°F	(93°C)	average	
	lbf	(kN)	lbf	(kN)	lbf	(kN)
1	10500	(47)	13000	(58)	11750	(52)
2	11700	(52)	10000	(44)	10850	(48)
3	9900	(44)	9500	(42)	9700	(43)
4	9000	(40)	9300	(41)	9150	(41)
5	12300	(55)	11500	(51)	11900	(53)
6	11900	(53)	11500	(51)	11700	(52)
7	11500	(51)	9800	(44)	10650	(47)
8	4000	(18)	3000	(13)	3500	(16)
9	10700	(48)	9000	(40)	9850	(44)
10	11600	(52)	11600	(52)	11600	(52)
11	12000	(53)	13000	(58)	12500	(56)

curves with increasing time. At some time, the specimen becomes saturated; beyond that point the slope of the rupture curve may remain constant. It is not clear that this point was reached with any of the samples tested in this program. This may require test times in excess of several thousand hours and correspondingly reduced test loads.

The finite time required for significant amounts of water to permeate the interior of a 1/2-in (13-mm) rod serves, in effect, like an incubation period. The existence of this incubation period explains why short-time stress-rupture tests (e.g., 100 h or less) have failed to show any significant effect of humidity on the stress-rupture strength of glass-reinforced rod and rope products [5].

The amount of water that is diffused into the interior of the rod is limited by (among other things) the amount that is adsorbed on the surface. The extent of adsorption of water vapor is markedly reduced by increasing the temperature [25, 26]. This explains why, after the incubation period, the stress-rupture strengths of the rod products decreased more rapidly at 160°F (71°C) than at 200°F (93°C). On the basis of this argument alone it might be surmised that the stress-rupture properties under high humidity would be very poor at room temperature, but this is not the case, both because the diffusion of water is relatively slow at room temperature and because room-temperature water is not nearly so damaging to glass-reinforced-plastic composites as hot water [24]. This was confirmed by one stress-rupture tests on a pultruded rod specimen which was maintained at room temperature and saturated humidity [27].

5. ANALYSIS AND DISCUSSION OF RESULTS

The effects of the nine variable process parameters, on the properties of the rods, were calculated by applying the evaluation procedures (Table 9) to the average low-speed tensile breaking load values (Table 12) and to the average estimated stress-rupture load values (Table 13). The results of these evaluations are given in Table 14. This table shows, for example, that collimation of the rovings during the pultrusion process raised the tensile breaking load of the rod by an average of 1300 lbf (6 kN) and the 100-h stress-rupture load by an average of 800 lbf (4 kN).

It may be seen that four of the process parameters appeared to be beneficial to both the tensile strength and the stress-rupture strength, namely, collimation and ultrasonic agitation of the rovings, increased end count, and post cure of the rod. It appears likely therefore, that the collimation process was successful in achieving a better alinement of the fibers, and that ultrasonic agitation did improve the wetting of the fibers. As expected, post curing was beneficial to both strength and weatherability. The potential benefits of pultruding a large number of small end-count rovings (i.e., more uniform distribution of fibers) were apparently negated by the operational difficulties of avoiding entanglements and obtaining good alinement with a large number of rovings.

Two of the process parameters appeared to be detrimental to both the tensile strength and the stress-rupture strength, namely, increased immersion length and the wetting agent additive. The detrimental effect of increased immersion length is puzzling; an explanation is not immediately

TABLE 14

EFFECTS OF THE VARIABLE PROCESS PARAMETERS ON ROD PROPERTIES, RUNS 1 - 11

Parameter	Incremental effect on tensile breaking load lbf	(kN)	100-h stress-rupture load lbf	(kN)
Preheat	+ 100	(+ 0.4)	- 900	(- 4.)
Collimation	+1300	(+ 6.)	+ 800	(+ 4.)
Post cure	+ 500	(+ 2.)	+1600	(+ 7.)
Twist	- 800	(- 4.)	+1500	(+ 7.)
End count	+1900	(+ 8.)	+2100	(+ 9.)
Tension	-3400	(-15.)	+2400	(+11.)
Immersion length	-1300	(- 6.)	- 900	(- 4.)
Ultrasonics	+ 500	(+ 2.)	+1700	(+ 8.)
Wetting agent	- 800	(- 4.)	-2800	(-12.)

apparent. The wetting agent undoubtedly facilitated wetting but, presumably, diminished the quality of the fiber/matrix interfacial bond.

Twisted rovings and added tension were both found to be beneficial to the rupture strength but detrimental to the tensile strength. The lesser degree of catenary and fuzz in twisted rovings presumably resulted in a better collimation of the rovings but, at the same time, in the twisted condition the tensile strength of the glass fibers was impaired. Added tension also contributed to better collimation but may have left a residual tensile stress in the fibers of the rod product.

The effect of preheating the rovings was found to be relatively insignificant, possibly because the ambient relative humidity during the manufacture of these samples was relatively low (less than 40 percent).

No meaningful correlation was found between the tensile breaking load values and the 100-h stress-rupture load values. Similarly, there is no apparent correlation between either of these two quantities and any of the properties given in Table 11. On the other hand, as shown in Figure 14, there does appear to be some correlation between transverse tensile strength and wet breakdown voltage, both of which are influenced by the quality of the fiber/matrix bond.

Comparison of the tensile breaking loads obtained at the two crosshead speeds (Table 12) shows that the maximum loads are significantly greater at high loading rates than at normal testing speeds. This suggests that breaking strength data for glass-reinforced-plastic rod products are not entirely meaningful unless accompanied by information regarding the speed of loading.

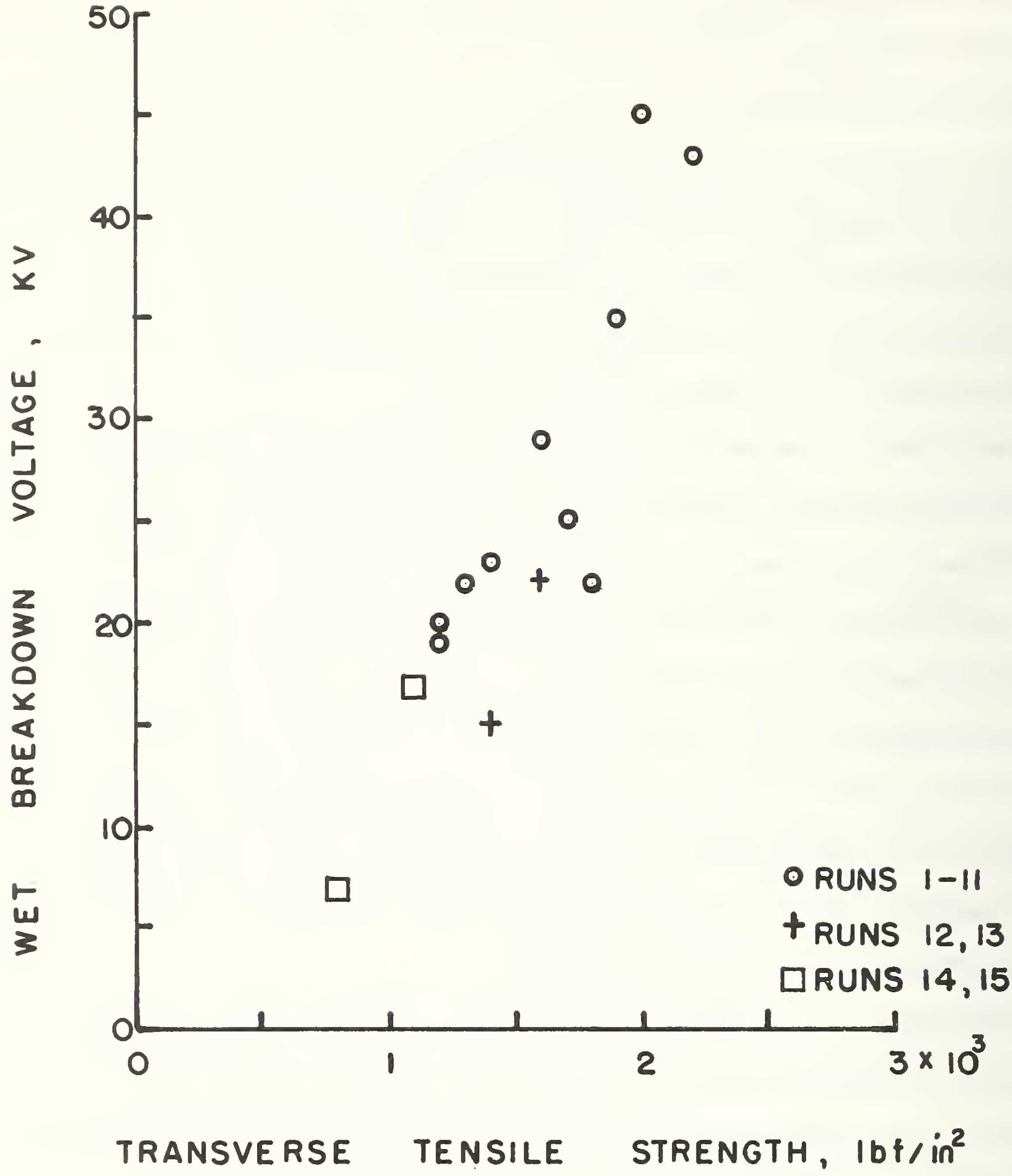

Figure 14 - Wet Breakdown Voltage Versus Transverse Tensile Strength
(1 lbf/in^2 = 6.89 kPa)

SECTION VI

PARAMETER STUDY OF THE MANUFACTURING PROCESS, PART II

1. EXPERIMENTAL MATERIALS

Two additional 1/2-in (13-mm) diameter rod samples (Runs 12 and 13) were pultruded from E-glass roving and the isophthalic polyester resin system. The processing conditions for Run 12 were selected with the intention of optimizing the long-term weatherability of the rod. Using the stress-rupture strength under conditions of elevated temperature and saturated humidity as the laboratory index of long-term weahterability, Table 14 indicates, in principle, what the processing conditions should be. In practice, this optimum combination of the variable processing parameters could not be employed with the available manufacturing facilities. Specifically, the special equipment required to introduce collimation is not readily compatible with the special equipment required to introduce additional tension into the rovings. Also, the collimating equipment constrains the rovings to a path which is too far below the resin surface in the dip trough to permit the ultrasonic horn to be used. Furthermore, as described earlier, attempts to use ultrasonic agitation in combination with added tension in the rovings introduces overheating problems, particularly when the standard-length dip trough is used. Accordingly, the following values of the nine variable processing parameters were selected for Run 12. These represent a compromise between the ideal combination, as indicated by the results given in Table 14, and the limitations of the available manufacturing facilities.

Roving preheat:	no	Immersion length:	std
Roving twist:	yes	Ultrasonic agitation:	no
Roving end count:	60	Collimation:	no
Roving tension:	yes	Post cure:	yes
Wetting agent:	no		

621082 95

The three constant processing parameters (resin viscosity, pulling speed and die temperature) were unchanged from those used in Runs 1 through 11, and the resin system formulation was the same as that used for those earlier samples which did not employ the wetting agent.

The singular lack of success which was achieved with the wetting agent in Runs 1 through 11 led to a decision to use Run 13 to evaluate the benefits of adding a coupling agent, rather than a wetting agent, to the resin system. The coupling agent selected for this purpose is a commercially available, cationic methacrylate functional silane having typical properties as shown in Table 15. The settings of the other process parameters for Run 13 were the same as those listed above for Run 12. The resin system formulations for the two runs are given in Table 16 and the operating conditions are given in Table 17.

2. TEST RESULTS AND ANALYSIS

The samples from Runs 12 and 13 were subjected to the same types of tests as had been used for Runs 1 through 11. The results of these tests are summarized in Table 18. Detailed data from the tensile and stress-rupture tests are given in the Appendix and the relationship between transverse tensile strength and wet breakdown voltage is shown in Figure 14.

Unfortunately, the rods were somewhat bowed as received from the manufacturer, presumably because they had been inadequately supported during the post-curing operation. This caused longitudinal splitting, or delamination, to develop in the tensile tests prior to total failure. It is felt that this splitting promoted the initiation of premature failures in the end fittings. Nevertheless, the highest load attained with the

TABLE 15

TYPICAL PROPERTIES OF SILANE COUPLING AGENT[a]

Percent Solids:	50.
Solvents:	Mostly diacetone alcohol.
Color:	Amber brown.
Refractive index at 77°F (25°C):	1.457.
Specific gravity at 77°F (25°C):	1.06.
Viscosity at 77°F (25°C):	0.74 poise (0.074 Pa·s).
Flash point, open cup:	130°F (54°C).
Suitable diluents:	Alcohols, water.

(a) According to the manufacturer.

TABLE 16

RESIN SYSTEM FORMULATION, RUNS 12 AND 13

	Run 12	Run 13
	wt (mass) pct	wt (mass) pct
Monostyrene	4.91	4.89
Peroxide catalyst	0.73	0.74
Die lubricant	0.92	0.93
Ultraviolet inhibiter	0.13	0.13
Coupling agent	-	0.30
Isophthalic polyester resin	Bal.	Bal.

TABLE 17

OPERATING CONDITIONS FOR MANUFACTURE OF RUNS 12 AND 13

Run No.	No. of rovings	Glass content	Ambient relative humidity	S-bend spacing[a]		Resin temperature
		wt (mass) pct	percent	in	(mm)	
12	24	75.4	37-39	5,3	(130,80)	(b)
13	24	75.6	39-40	5,3	(130,80)	(b)

(a) See Table 10.

(b) Ambient

621082

TABLE 18

DIMENSIONS AND PROPERTIES SUMMARY, RUNS 12 AND 13

	Run 12	Run 13
Diameter, in	0.497	0.497
(mm)	(12.6)	(12.6)
Density, lb/in^3	0.0721	0.0721
(Mg/m^3)	(2.00)	(2.00)
Weight (mass), lb/ft	0.168	0.168
(kg/m)	(0.250)	(0.250)
Rockwell hardness (Scale E)	67	60
Transverse tensile strength, lbf/in^2	1600	1400
(MPa)	(11)	(10)
Wet breakdown voltage, kV	22	15
Tensile **breaking load,**		
conventional, lbf	26750	25250
(kN)	(119)	(112)
high-speed, lbf	34500	33000
(kN)	(153)	(147)
100-h stress-rupture load, estimated,		
at 160°F (71°C), lbf	12300	11300
(kN)	(55)	(50)
at 200°F (93°C), lbf	12250	11000
(kN)	(54)	(49)
average, lbf	12300	11150
(kN)	(55)	(50)

Run 12 specimens at normal speeds is close to the calculated breaking load for this run, which is 26100 lbf (116 kN).* Comparison of the breaking loads for Run 13 with those for Run 12 (Table 18) shows that the coupling agent additive in Run 13 was ineffective, at best, insofar as the tensile breaking load is concerned.

In the high-speed tensile tests the failures also appeared to have initiated in the end fittings. However, just as with Runs 1 through 11, the breaking loads in the high-speed tests are significantly greater than those achieved in the conventional tensile tests.

Some delamination due to bowing was also experienced in the stress-rupture tests but the conclusion is nevertheless clear (Table 18) that the coupling agent additive in Run 13 was detrimental to the stress-rupture strength.

The average 100-h stress-rupture load for Run 12, 12300 lbf (55 kN), is considerably less than the calculated value (from Tables 13 and 14). It is, however, approximately equal to the 100-h stress-rupture load for Run 11 (12500 lbf, 56 kN) which was the highest of all. It is evident, therefore, that the various process parameters are not independent in terms of their effects on stress-rupture strength, which is the way they were treated in the design of the experiment. In other words, if the advantages of using twisted roving, a high end count and added tension result from

---

*This calculation is straightforward. Starting, for example, with the conventional breaking load for Run 1 (Table 12), the breaking load for Run 12 is found by algebraically adding to this value the breaking load increments for tension and post cure (Table 14).

their tendencies toward less entanglement and better fiber collimation, it follows that the benefits of using the three together would not necessarily be linearly additive. Perhaps 12500 lbf (56 kN) is about the limit of the improvement in stress-rupture capacity that can be attained with this resin/fiber combination through modification of the process parameters. If this is so, further improvements, if any, would have to come from changes in the consitituent materials of the rod.

Although this program was concerned primarily with mechanical properties, it is interesting to note the wide differences that were observed in the average wet breakdown voltages of the different samples (Fig. 14). These ranges from 45 kV for rod from Run 8 to 15 kV for rod from Run 13. Largely as a matter of curiosity, the average breakdown voltages of samples from these two runs were measured again, this time using dry specimens. Interestingly, the average dry breakdown voltages were found to be nearly equal; 64 kV for Run 8 and 62 kV for Run 13. It thus appeared that the process parameters have no significant effect on dry breakdown voltage. This conclusion was supported by subsequent tests on specimens from Run 1 which exhibited an average dry breakdown voltage of 67 kV.

SECTION VII

VARIATION OF THE CONSTITUENT MATERIALS

1. SELECTION OF THE CONSTITUENT MATERIALS

This part of the program was designed to evaluate the additional improvements in the weatherability of the pultruded rod product introduced by changing the fiber and matrix constituents. To this end, selection of a non-metallic fiber material and a matrix resin, which exhibit greater moisture resistance than E-glass and isophthalic polyester, was desired. Largely on the basis of the manufacturer's claims, aramid was selected as the fiber material. According to these claims, aramid fiber experiences no reduction in tensile strength as a result of 24-h immersion in water, and less than a four-percent decrease in the interlaminar shear strength of unidirectional aramid-fiber composites following a 90-day exposure to high humidity at 120°F (49°C). It has also been reported [28, 29] that the stress-rupture strength of aramid/epoxy strands is superior to that of glass/epoxy strands.

A small, preliminary sample of 1/4-in (6-mm) diameter rod was pultruded from a quantity of reject-grade aramid fiber and the isophthalic polyester resin. Tensile tests on specimens of this rod (see Appendix) revealed satisfactory short-time strength but the appearance of the fractured specimens suggested that the fibers had been only partially wetted by the resin. This observation was confirmed by tests conducted by the aramid fiber manufacturer. These tests showed that aramid/isophthalic composites exhibit poor interlaminar shear strengths. These tests also suggested two other resin systems which provide substantially higher shear strengths in combination with aramid fiber. One of these, a propoxylated bisphenol-A fumarate polyester, has been used as the matrix material for a glass mat composite that exhibited relatively little degradation of tensile strength after two years in a hot, humid climate [30]. This fact, together with other data that attribute higher weather resistance to polyester composites than to epoxy composites [31], led to the selection of the bisphenol fumarate polyester as the resin system to be used in this part of the program.

It should be mentioned that what, to the eye, appears to be poor wetting of the aramid fibers is not apparent in photomicrographs of aramid-fiber composites [28, 32]. These photomicrographs do not show voids around the fibers, even under magnifications of 2000. It might be speculated that the fibers are, in fact, wetted by the resin but that the quality of the bond is destroyed during the cooling process following curing as a result of the aramid fiber's negative coefficient of thermal expansion [33].

The characteristics of the bisphenol fumarate polyester resin and the aramid fiber that were used in this program are given in Tables 19 and 20, respectively.

2. MANUFACTURE OF EXPERIMENTAL MATERIALS

Two 1/2-in (13-mm) diameter samples, Runs 14 and 15, were manufactured. Run 14 was pultruded with the bisphenol fumarate polyester resin and the same E-glass fiber that had been used for the previous samples. Run 15 was pultruded with the bisphenol fumarate polyester resin and aramid fiber.

In order to derive the most useful information from the results, the processing conditions for the two samples should be similar to each other and to those used for Run 12. (Run 12, it will be recalled, was designed to "optimize" the weatherability of the E-glass/isophthalic combination.) However, practical considerations necessitated some differences in the settings of both the variable process parameters and the "constant" process parameters.

TABLE 19

CHARACTERISTICS OF BISPHENOL FUMARATE POLYESTER RESIN[a]

Monomer:	Styrene, 33 percent.
Viscosity:	110 - 150 poise (11 - 15 Pa.s) at 77°F (25°C)
Specific gravity:	1.08.
Storage life:	6 months at 75°F (24°C)

(a) According to the manufacturer.

TABLE 20

CHARACTERISTICS OF ARAMID FIBER ROVING[a]

Type:	Commercial grade, continuous.
Specific gravity:	1.45.
Fibers per strand:	1000.
End Count[b]	10.
Roving denier[c]:	14200.
Fiber diameter[d]:	0.00046 in (12 um).
Twist:	None.
Finish:	None.
Tensile strength[e]:	525,000 lbf/in^2 (3620 MPa).
Tensile modulus[e]:	19 x 10 lbf/in^2 (130 GPa).

[a] According to the manufacturer, except as noted.

[b] Number of strands per roving.

[c] Mass in grams of 9000 meters, by definition.

[d] Calculated.

[e] Per ASTM Designation D-2343 [18].

a. Variable Process Parameters. Data acquired in the course of another Air Force program [34] showed that pre-drying of aramid fiber is absolutely essential to achieve good wetting by the resin. Accordingly, the rovings for Runs 14 and 15 were preheated. This had not been done for Run 12. The form of aramid roving that was recommended by its manufacturer for this application (10-end, untwisted) did not match the "optimum" form of E-glass roving (60-end, twisted). In view of these considerations the following settings of the variable process parameters were selected for Runs 14 and 15:

	Run 14	Run 15
Roving preheat	yes	yes
Roving twist	yes	no
Roving end count	60	10
Roving tension	yes	yes
Wetting agent	no	no
Immersion length	std	std
Ultrasonic agitation	no	no
Collimation	no	no
Post cure	yes	yes

It has been reported [35] that abrasion produces a decrease in the compressive yield strength of aramid yarn. Therefore, to minimize the possible effects of abrasion damage on the pultruded rovings, the rods which form the tension S-bend (Fig. 10) were mounted in ball bearings for Run 15. During the pultrusion process these rods were observed to rotate freely. Thus, while abrasion damage was probably avoided, the degree of tension introduced into the rovings was probably reduced.

b. Constant Processing Parameters. In the manufacture of Runs 1 through 13, the settings of three processing parameters were maintained constant, i.e., resin viscosity, pulling speed and die temperature. The different cure characteristics of the bisphenol fumarate polyester resin, as compared with the isophthalic polyester resin, necessitated some changes in these processing parameters for the manufacture of Runs 14 and 15.

The bisphenol fumarate polyester was found to have a higher polymerization exotherm. Thus, at a pulling speed of 12 in/min (5 mm/s) (which had been used for Runs 1-13) boiling styrene vapors ruptured or otherwise damaged the rod as it emerged from the die. Attempts to correct this by changing the catalyst concentration had the effect of increasing the gel time to unacceptable levels without significantly lowering the exotherm. The pulling speed was, therefore, lowered to 6 in/min (3 mm/s) for Runs 14 and 15.

The bisphenol fumarate polyester resin was thinned with monostyrene to provide the required viscosities. In the case of Run 14, the resin system viscosity was in the same range as had been used for the pultrusion of Runs 1 through 13. The difficulties in wetting aramid fiber, however, necessitated a further reduction in viscosity for Run 15 in order to obtain good surface quality on the pultruded rod. The resin system formulations for Runs 14 and 15, and the resultant viscosities, are given in Table 21.

c. Operating Conditions. The operating conditions for the manufacture of Runs 14 and 15 are given in Table 22. Although the individual fiber diameters of E-glass and aramid are nearly equal, each E-glass roving contained 24000 fibers while each aramid roving contained only 10000 fibers, and this is reflected in the difference in the number of rovings

TABLE 21

RESIN SYSTEM FORMULATION AND VISCOSITY, RUNS 14 AND 15

	Run 14 wt (mass) pct	Run 15 wt (mass) pct
Monostyrene	19.20	22.15
Peroxide catalyst	0.49	0.49
Die lubricant	0.93	0.93
Ultraviolet inhibitor	0.13	0.14
Bisphenol fumarate polyester	Bal.	Bal.
Viscosity at 77°F, poise (Pa·s)	12.1 (1.21)	7.9 (0.79)

TABLE 22

OPERATING CONDITIONS FOR MANUFACTURE OF RUNS 14 AND 15

Run No.	14	15
Fiber type	E-glass	aramid
No. of rovings	25	58
Fiber content, wt (mass) pct vol pct	78.8 61.5[a]	60.6[a] 53.0[a]
Ambient relative humidity, pct	23-27	35-37
S-bend spacing[b], in (mm)	5,3 (130,80)	5,3 (130,80)
Resin temperature	(c)	(c)

(a) Calculated.

(b) See Table 10.

(c) Ambient, approximately 73°F (23°C)

required for each run. Nevertheless, the fiber content of the aramid rod had to be made less than that of the glass rod because of the difficulties in wetting the aramid fiber. The ignition loss test for measuring fiber content could not be applied to the aramid rod so the fiber fractions shown in the table for this product were calculated. Since the density of aramid is only about 60 percent of the density of E-glass, volume fractions of fiber content provide a more meaningful comparison between the two samples than weight fractions, and these data are included in the table.

3. TEST RESULTS AND ANALYSIS

Specimens from Runs 14 and 15 were subjected to the same types of tests as had been used on the previous samples. The results are summarized in Table 23. Data for Run 12 are included to facilitate comparisons. Detailed data from the tensile and stress-rupture tests are given in the Appendix.

As expected, the density of the aramid-reinforced rod is less than two-thirds of that of the glass-reinforced rods. The hardness of the glass/isophthalic rod is 67 on the Rockwell E scale. (All of the post-cured glass/isophthalic samples had hardnesses of 60 or more.) Changing to the bisphenol fumarate resin reduced the hardness to 45, and adding aramid fiber in place of glass produced a further reduction to 34. A similar trend is noted for the transverse tensile strength and the wet breakdown voltage. As shown in Figure 14, however, the relationship between transverse tensile strength and wet breakdown voltage is maintained. The average dry breakdown voltage was measured on specimens from Run

TABLE 23

DIMENSIONS AND PROPERTIES SUMMARY, RUNS 12, 14 AND 15

	Run 12	Run 14	Run 15
Fiber	E-glass	E-glass	aramid
Resin[(a)]	IPR	BFPR	BFPR
Diameter, in	0.497	0.496	0.489
(mm)	(12.6)	(12.6)	(12.4)
Density, lb/in^2	0.0721	0.0718	0.0464
(Mg/m^3)	(2.00)	(1.99)	(1.28)
Weight (mass), lb/ft	0.168	0.167	0.105
(kg/m)	(0.250)	(0.249)	(0.156)
Rockwell hardness (Scale E)	67	45	34
Transverse Tensile strength, lbf/in^2	1600	1100	700[(b)]
(MPa)	(11)	(8)	(5)[(b)]
Wet breakdown voltage, kV	22	17	8
Tensile breaking load,			
conventional, lbf	26750	28750	27650
(kN)	(119)	(128)	(123)
high-speed, lbf	34500	35000	30000
(kN)	(153)	(156)	(133)
100-h stress-rupture load, estimated,			
at 160°F (71°C), lbf	12300	12400	15200
(kN)	(55)	(55)	(68)
at 200°F (93°C), lbf	12200	12800	17000
(kN)	(54)	(57)	(76)
average, lbf	12300	12600	16100
(kN)	(55)	(56)	(72)

(a) IPR (isophthalic polyester resin); BFPR (bisphenol fumarate polyester resin)

(b) Value is questionable; diametral compression specimens deformed substantially before failure.

15 and found to be only 37 kV, whereas glass/isophthalic rods exhibit dry breakdown voltages of 60 kV or more. The low transverse tensile strength and the low breakdown voltages for the aramid-reinforced rod are attributed to the relatively poor wetting of the fiber by the matrix resin.

a. Tensile Properties. Examination of the tensile breaking loads in Table 23 shows that these values are not greatly affected by changing from glass fiber to aramid fiber or by changing from isophthalic to bisphenol fumarate polyester. Perhaps the only significant effect to be noted is that the aramid-reinforced rod did not exhibit the marked increase in strength at high loading rates that was observed with the glass-reinforced rods. It should also be pointed out that in the conventional tensile tests of the aramid-reinforced specimens all failures occurred inside an end fitting. In this case this behavior is believed to be due, only in part, to the comparatively low shear strength of the rod product. A major cause for the inability to attain the full strength of the aramid-reinforced rod is believed to lie in the inadequacy of the H3M end fittings. These fittings, it will be recalled, were developed specifically for glass-reinforced products. The design of an efficient end fitting for aramid-reinforced rod would have to be tailored to the elastic and deformational characteristics of that material.

The mode of failure of the aramid-reinforced rod specimens in tension also merits comment. Whereas glass-reinforced rods shatter upon tensile failure, with all of the fibers brooming out explosively, the aramid-reinforced rod specimens remained relatively intact apart from the fracture location. However, the recoil from the tensile fracture generally caused the specimens to buckle compressively at another location along the length of the rod and numerous compressive shear cracks developed on the surface. See Figure 15. This unusual behavior is believed to result from the relatively poor compressive strength properties that have been reported for aramid fiber [36, 37].

The fact that Table 23 shows only minor differences in tensile breaking load is only incidental to this program. The new fiber and resin constituents that were used in Runs 14 and 15 were primarily selected to give improved weatherability, i.e., increased stress-rupture life under moist conditions.

b. Stress-Rupture Properties. Several of the test specimens from Run 14 developed longitudinal cracks during stress-rupture testing. These seemed to be due to swelling of the specimens, as a result of the absorption of moisture from the saturated-humidity environment, despite other data which suggest that bisphenol polyesters should be less susceptible to this type of damage than isophthalic polyesters [38]. The presence of the longitudinal cracks did not appear to affect the load-carrying capability of the specimens and, in fact, the 100-h stress-rupture capacities for Run 14 were slightly greater than those for Run 12 (Table 23).

The stress-rupture data for the specimens from Runs 14 and 15 exhibited the same unusual characteristics as those for the glass/isophthalic specimens, namely, (1) the slopes of the rupture curves became increasingly negative with increasing time, and (2) the stress-rupture strength tended to be greater at 200^{o}F than at 160^{o}F, particularly at long rupture times. From this it might be inferred that these phenomena are not limited to

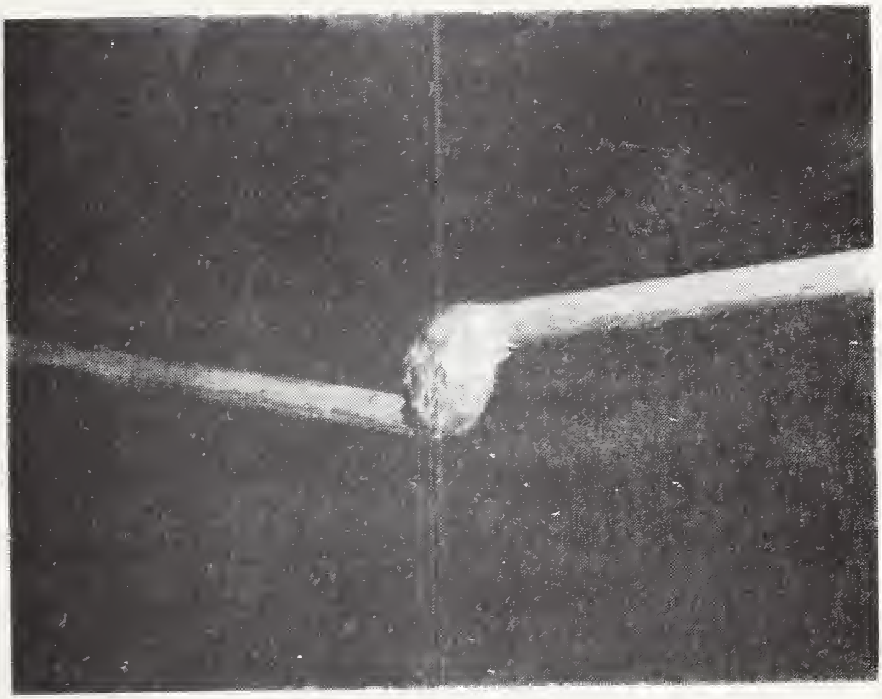

Figure 15 - Compressive Buckle in an Aramid FRP Rod, Produced by the Recoil from a Tensile Failure at another Location on the Rod

specific types of resin matrices and fiber reinforcements. Rather, it would appear that the critical region is the fiber/matrix interface, which tends to support the stress-rupture analysis given in Section 5.4.3.

Table 23 shows that the use of aramid-fiber reinforcement produced a striking improvement in stress-rupture properties as compared with glass-fiber reinforcement. This suggests that the weatherability of the aramid-reinforced rod under moist conditions may be expected to be substantially superior to that of glass fiber-reinforced rod.

SECTION VIII

DISCUSSION AND RECOMMENDATIONS

The principal objective of this program was the development of a pultruded, non-metallic rod material with enhanced strength, over currently available rods, under long-time exposure to moist environments. In pursuing this objective the greatest emphasis was placed on the improvements that could be achieved through modification of the manufacturing process parameters. Nevertheless, the degree of improvement that was attained in this way was relatively small. The test results suggest that while individual process parameters may have significant effects on the weatherability of the product, the effects of optimizing several such parameters are not lineraly cumulative, and the total improvement that was obtained in this way is less than impressive. In fact, the properties of the glass FRP rod which was manufactured with the "optimum" combination of the process parameters (Run 12) are not especially noteworthy in comparison with the properties of some commercially available products [5].

This finding may indicate that the manufacturers of high-performance pultrusions have already optimized their processes; not necessarily by means of formal research programs but, rather, through regular observation of product characteristics as they are influenced by day-to-day variations in the manufacturing process. It is also possible that the present study did not explore the individual process parameters in sufficient depth. Only two settings of each process parameter were examined whereas a thorough understanding of the effects of each parameter would require a more intensive investigation. For example, it was found that 60-end glass rovings provide an improvement in this application over 30-end rovings. Would 120-end rovings furnish an additional improvement? The data are inadequate to provide a definitive answer to this question.

Although the parameter study of the manufacturing process did not lead to major improvements in the rod product, it did lead to the development of several new test methods and testing techniques which have potential value for future R&D programs. These accomplishments, and others, are summarized in the next section of this report.

In contrast to the magnitude of the study devoted to the manufacturing process, a relatively small effort was directed toward an investigation of the benefits that could be derived from changes in the material constituents of the rod. Yet, the payoff was substantial. It was found that the stress-rupture strength of rod fabricated from aramid fiber and bisphenol fumarate polyester resin is about thirty percent higher than that of "optimized" E-glass/isophthalic polyester rod, under high heat and humidity. Since the aramid FRP rod was manufactured without full knowledge of the effects of the process parameters on the properties of this material, it would seem that further improvements could be realized by optimizing some of these parameters, such as end count, coupling agent, etc.

On the basis of these results it would seem that a significantly improved non-metallic antenna-support material was developed. However, several words of caution are in order.

It remains to be seen whether the results of stress-rupture tests under high heat and humidity can, in fact, serve as measures of weatherability. This premise is being tested now by the installation of several aramid FRP guys, similar to the rod manufactured in Run 15, on antenna towers in Colorado and Hawaii (NBS radio stations WWV and WWVH, respectively).

Another cause for concern is the low compressive strength of aramid FRP rod. Although antenna-support materials are primarily tension members, compressive bending stresses introduced during handling, shipping, storage and installation could, perhaps, cause damage. For example, it is calculated that 1/2-in (13-mm) diameter aramid FRP rod may not be coiled to diameters of less than 11 ft (3.4 m) lest compressive failure result. This is far in excess of the diameters to which glass FRP rod may safely be coiled. It would appear that storage tests, similar to those that have been carried out on glass FRP rod products [5], should be performed to establish the safe limits of coil diameter and storage temperature for aramid FRP rod. Similarly, the flexural strength under low temperatures and the resistance to transverse vibration should be checked for aramid FRP rod, as has been done for glass FRP rod [5].

Finally, the electrical characteristics of aramid FRP rod merit further study, particularly for applications where the rods may be exposed to high voltages and strong electromagnetic fields. The dielectric strength of aramid FRP rod was examined only cursorily in the present program and the results were less than encouraging.

SECTION IX

SUMMARY AND CONCLUSIONS

Fifteen experimental samples of pultruded FRP rod were manufactured and tested in this program to develop a non-metallic antenna-support material with improved weatherability. Thirteen of these samples were used to explore the effects of modifications of the pultrusion process (Sections V and VI). These samples were designed on the basis of a survey of the pultrusion processes used by manufacturers of glass FRP rod (Section II.1) and an examination of the deficiencies in existing glass FRP rod products (Section II.2). The other two samples were used to explore the effects of changes in the material constituents of the rod (Section VII). The results of elevated-temperature stress-rupture tests, under saturated humidity conditions, were used as the laboratory measure of weatherability.

It was found that modifications of the pultrusion process can, indeed, improved the weatherability of glass FRP rod. Each of the following modifications were found to raise the 1-0-hour stress-rupture strength by more than ten percent under high heat and humidity:

adding tension in the rovings,
using a roving end count of 60 rather than 30,
using twisted rather than untwisted rovings,
ultrasonically agitating the rovings in the dip trough, and
post curing the rod.

Collimating the rovings during passage through the dip trough resulted in a lesser improvement. Of these modifications, only the addition of tension in the rovings produced a simultaneous reduction of more than ten percent in the short-time tensile strength of the product.

The following modifications were found to reduce the 100-hour stress-rupture strength of glass FRP rod:

increasing the immersion length of the rovings in the dip trough,
adding a polycaprolactone wetting agent to the resin, and
adding a silane coupling agent to the resin.

Unfortunately, major improvements in weatherability (i.e., 30 percent or more) could not be achieved by using all of the beneficial modifications simultaneously, partly because limitations of the manufacturing facilities did not permit all of the beneficial modifications to be used simultaneously, and partly because the improvements attributable to each modification were not linearly cumulative when used in combination. As a result, the weatherability of glass FRP rod was not significantly improved here over the weatherability of certain high-performance glass FRP rod products that are commercially available at this time.

In that part of this program in which different material constituents were examined, changing from an isophthalic polyester resin system to a bisphenol fumarate polyester resin system produced only minor improvements in the 100-hour stress-rupture strength of glass FRP rod under high heat and humidity. However, replacing the E-glass fiber with aramid fiber yielded a striking, 30-percent improvement in the 100-hour stress-rupture strength under high heat and humidity. The short-time tensile strength was not significantly different from that of glass FRP rod despite the fact that the fiber volume-fraction of the aramid FRP rod was less than that of high-performance glass FRP rod (53 percent vs 61 percent). The properties of the aramid FRP rod were even more impressive on a strength/weight basis since the density of this product was less than two-thirds of that of glass FRP rod. It is logical to expect that a parameter study of the pultrusion process for aramid FRP rod -- similar to that which was conducted here for glass FRP rod -- could lead to further improvements in the aramid FRP rod.

Despite these promising results, aramid FRP rod cannot be recommended for antenna-support applications without additional study. There is an indicated need for further testing and evaluation of certain peripheral properties that were only examined cursorily in this program (Section VIII).

During the course of this investigation a number of other accomplishments and conclusions were recorded which have potential value in future R&D studies and applications. These include:

1. Two new potted end fittings for glass FRP rod were developed which are superior, in several respects, to a variety of commercial end fittings with which they were compared. These new fittings, which are generally capable of achieving the full tensile strengths of available glass FRP materials, include a shear-type fitting (Mod 4) and a compression-type fitting (H3M) (Section IV). The method by which these fittings were developed is believed to be applicable to the development of a high-performance end fitting for aramid FRP materials, as well.

2. A high-speed tensile test method for FRP rod products was developed (Section III.1). Through the use of this method it was shown that the tensile strength of glass FRP rod is substantially greater at high loading rates than at conventional loading rates (Table 12). This rate effect was not apparent for the aramid FRP rod.

3. Two test methods were developed which furnish indirect evidence of the quality of the fiber/matrix interface in FRP rod. One of these, a diametral compression test (Section III.7), provides a measure of the transverse tensile strength of the rod, which is believed to be influenced by the tensile strength of the interfacial bond. The second test method measures the electrical breakdown voltage of wet FRP rod samples, which is believed to be influenced by the contiguity of the fiber/matrix interface (Section III.5). A correlation between the results of these two tests methods was established (Fig. 14).

4. A series of six 30000-lbf (130-kN) capacity creep-testing machines was designed and fabricated. These machines, which incorporate a 100:1 compound-lever system, will accommodate test specimens up to nine feet (3 m) long and are equipped with environmental chambers for use to 200^{o}F (93^{o}C) under saturated humidity conditions (Section III.2).

5. The stress-rupture behavior of FRP rod, under high humidity, was found to exhibit unusual temperature and time characteristics.

This behavior was explained in terms of the opposing effects of temperature on two time-dependent processes which govern the transport of moisture from the environment to the fiber/matrix interface (Section V.4.C)

APPENDIX

1. TENSILE TEST RESULTS, RUNS 1-11

The results of the tensile tests at a crosshead speed of 0.75 in/min (0.32 mm/s) are given in Table A.1. Except as otherwise noted, each specimen was fitted with H3M end fittings using cruciform wedges and C2W3 potting compound, and had a free length between 52 and 62 in (1.3 and 1.6 m). Also given in Table A.1 is the average breaking load for each run. In general, this was calculated by averaging the maximum loads that were attained with specimens that failed in their free lengths. However, this procedure could not be applied to the results from Runs 3 and 7 because, in these cases, failures in the free lengths were not obtained. Run 3 was one of the runs which utilized the wetting agent, which turned out to be a very effective low-profile additive, and this, together with a long immersion time and ultrasonic agitation, produced a rod with an extremely slick outer surface which could not be adequately gripped. Four tensile tests resulted in four pullouts. The average breaking load of Run 3 is, therefore, only estimated on the basis of the highest maximum load attained.

Two tensile tests on rod specimens from Run 7 resulted in failures which apparently initiated in an end fitting. The shortage of material from Run 7 precluded additional testing and the average tensile strength of this run is also estimated on the basis of the limited data obtained.

In calculating the average tensile strength for Run 10, the results of two tests, which had culminated in pullouts, were included in the average since the maximum loads in these two tests exceeded that obtained with one specimen which had failed in its free length.

In the first three high-speed tensile tests that were performed the failures appeared to initiate in an end fitting. Because of the viscoelastic nature of the C2W3 potting compound (which is normally used with H3M end fittings) it was surmised that the high loading rates were causing the potting compound to behave like a stiff material. Consequently, a new potting compound, C1W2, was formulated, which is more flexible than C2W3. Nevertheless, failure in most of the high-speed tensile tests appeared to initiate in an end fitting. The results of these tests are given in Table A.2. The free lengths of all specimens were 27 or 28 in (0.69 or 0.71 m) and, except as noted, all failures appeared to have initiated in an end fitting.

2. STRESS-RUPTURE TEST RESULTS, RUNS 1-11

The results of eighty-three rupture tests on rod specimens from Runs 1 through 11, at 160 and 200°F (71 and 93°C), are given in Tables A.3 and A.4, respectively. Each specimen was fitted with Type R/P commercial end fittings using cruciform wedges and C2W3 potting compound. Except as otherwise noted, each specimen failed in its free length within the temperature-humidity chamber.

3. TENSILE TEST RESULTS, RUNS 12 AND 13

The results of the tensile tests at a crosshead speed of 0.75 in/min (0.32 mm/s) are given in Table A.5. Each specimen was fitted with H3M end fittings using cruciform wedges and C2W3 potting compound and, except as otherwise noted, had a free length between 52 and 62 in (1.3 and 1.6 m).

The results of the tensile tests at a crosshead speed of 300 in/min (130 mm/s) are given in Table A.6. Here, too, each specimen was fitted with H3M end fittings using cruciform wedges but in this case the more flexible C1W2 potting compound was used. Nevertheless, all failures appeared to have initiated in an end fitting. The free lengths of all specimens were 27 or 28 in (0.69 or 0.71 m).

4. STRESS-RUPTURE TEST RESULTS, RUNS 12 AND 13

The results of thirteen stress-rupture tests on rod specimens from Runs 12 and 13 at 160 and 200°F (71 and 93°C) are given in Table A.7. Each specimen was fitted with Type R/P commercial end fittings using cruciform wedges and C2W3 potting compound. Except as otherwise noted, each specimen failed in its free length within the temperature-humidity chamber.

5. TENSILE TESTS ON PRELIMINARY SAMPLE OF 1/4-IN (6-mm) ARAMID/ISOPHTHALIC ROD

Six tensile tests were performed at room temperature using a crosshead speed of 0.75 in/min (0.32 mm/s). All of the specimen failures occurred in or adjacent to an end fitting. These were attributed to the low shear strength of the rod which prevented the effective transfer of load from the fittings to the interior of the rod specimens. The low shear strength was evident from the appearance of the failed specimens, which showed that the aramid fibers had been only sparsely wetted by the resin. The test results are given in Table A.8.

6. TENSILE TEST RESULTS, RUNS 14 AND 15

Fifteen tests were performed at room temperature. The results of twelve tests at a crosshead speed of 0.75 in/min (0.32 mm/s) are given in Table A.9; all of these specimens had free lengths of 47 or 48 in (1.2 m). The results of three tests at 300 in/min (130 mm/s) are given in Table A.10; these specimens had free lengths of 27 or 28 in (0.7 m).

7. STRESS-RUPTURE TEST RESULTS, RUNS 14 AND 15

Twenty-one stress-rupture tests were performed under saturated humidity conditions, eight at 200°F (93°C) and thirteen at 160°F (71°C). The results are given in Table A.11.

TABLE A.1

RESULTS OF CONVENTIONAL TENSILE TESTS, RUNS 1-11

Rod diameter: 1/2 in (13 mm), nominal.
Free length: 52 to 62 in (1.3 to 1.6 m), except as noted.
Crosshead speed: 0.75 in/min (0.32 mm/s).
End Fittings: H3M with cruciform wedges and C2W3 potting compound, except as noted.

Run No.	Specimen No.	Maximum load lbf	(kN)	Notes
1	R1Pc8B	29450	(138)	a
1	R1Pc3B	29000	(129)	a
1	R1Pc6B	28600	(127)	a
1	R1Pc8A	25300	(113)	a,b
1	Average	29000	(129)	
2	R2Pc5B	28700	(128)	a
2	R2Pc7B	20550	(91)	c
2	R2Pc1A	26550	(118)	d
2	R2Pc1B	29450	(131)	a
2	R2Pc4B	7150	(32)	c,e
2	Average	29100	(129)	
3	R3Pc1A	24650	(110)	c
3	R3Pc2A	11850	(53)	c
3	R3Pc2A	25250	(112)	c,f
3	R3Pc4A	27050	(120)	c
3	Average	27100	(121)	g
4	R4Pc3B	22950	(102)	a
4	R4Pc4A	21000	(93)	a
4	R4Pc8A	20000	(89)	d
4	R4Pc8B	10300	(46)	c
4	R4Pc8C	23550	(105)	a
4	Average	22500	(100)	
5	R5APc4A	23150	(103)	a
5	R5APc1B	22800	(101)	a
5	R5APc1A	18500	(82)	d
5	Average	23000	(102)	
6	R6Pc2B	20700	(92)	a
6	R6Pc2A	25450	(113)	a
6	R6Pc2C	28000	(125)	a
6	Average	24700	(110)	

(continued)

TABLE A.1 - (Continued)

Run No.	Specimen No.	Maximum load lbf	(kN)	Notes
7	R7Pc1A	25750	(115)	d
7	R7Pc1B	26150	(116)	d
7	Average	26200	(117)	g
8	R8Pc1A	25400	(113)	a
8	R8Pc2A	26750	(119)	a
8	R8Pc3A	25700	(114)	a
8	Average	25900	(115)	
9	R9Pc1A	27800	(124)	a
9	R9Pc2A	28150	(125)	a
9	R9Pc3A	26650	(119)	d
9	Average	28000	(125)	
10	R10Pc1A	30700	(137)	h
10	R10Pc2A	23750	(106)	c
10	R10Pc3A	31400	(140)	a
10	R10Pc4A	28400	(126)	a,i
10	R10Pc8A	31250	(139)	h,i
10	R10Pc7A	26100	(116)	a,j
10	Average	30400	(135)	
11	R11Pc5	28000	(125)	c
11	R11Pc1A	28150	(125)	a
11	R11Pc7B	30950	(138)	a
11	Average	29600	(132)	

Notes:

a. Failed in the free length.
b. Exposed to stress-rupture conditions prior to tensile test. (See Table A.3.) Result not included in the average.
c. Pulled out of end fitting. Result not included in the average.
d. Failure appeared to have initiated in an end fitting. Result not included in the average.
e. End fittings potted with C1W2 compound. Free length, 47 in (1.2 m).
f. Same specimen as above, retested with Mod 4 end fittings.
g. Estimated.
h. Pulled out of end fitting. Result included in the average.
i. Free length, 48 to 51 in (1.2 to 1.3 m).
j. Exposed to room-temperature stress-rupture conditions prior to tensile test [27]. Result not included in the average.

TABLE A.2

RESULTS OF HIGH-SPEED TENSILE TESTS, RUNS 1-11

Rod diameter: 1/2 in (13 mm), nominal.
Free length: 27 to 28 in (0.7 m).
Crosshead speed: 300 in/min (130 mm/s).
End fittings: H3M with cruciform wedges and potting compounds as noted.
All failures appeared to have initiated in an end fitting except as noted.

Run No.	Specimen No.	Potting Compound	Maximum load lbf	(kN)	Notes
1	R1Pc8C	C2W3	-	-	a
1	R1Pc7B	C1W2	36000	(160)	b
2	R2Pc7C	C2W3	34700	(154)	
2	R2Pc5D	C1W2	33200	(148)	
3	R3Pc1C	C1W2	33500	(149)	
3	R3Pc5A	C1w2	37000	(165)	
4	R4Pc6A	C1W2	29000	(129)	
4	R4Pc6B	C1W2	28500	(127)	
5	R5APc2B	C1W2	32500	(146)	
6	R6Pc6A	C1W2	38100	(169)	b
6	R6Pc6C	C1W2	17000	(76)	c
6	R6Pc9A	C1W2	35000	(156)	
8	R8Pc11A	C1W2	34000	(151)	
9	R9Pc5A	C1W2	36000	(160)	
10	R10Pc4C	C2W3	-	-	a
10	R10Pc3C	C1W2	-	-	a
10	R10Pc6A	C1W2	15000	(67)	c
10	R10Pc6B	C1W2	34000	(151)	
11	R11Pc2A	C1W2	32500	(145)	

Notes:

a. Maximum load not measured.
b. Failure appeared to have initiated in the free length.
c. Specimen pulled out of an end fitting.

TABLE A.3

RESULTS OF STRESS-RUPTURE TESTS AT 200°F (93°C) AND SATURATED HUMIDITY, RUNS 1-11

Rod diameter: 1/2 in (13 mm), nominal.
End fittings: Type R/P with cruciform wedges and C2W3 potting compound.
All failures occurred in the free length within temperature-humidity chamber, except as noted.

Run No.	Specimen No.	Test load lbf	(kN)	Time to rupture h	Notes
1	R1Pc6C	14000	(62)	0.5	
1	R1Pc4A	14000	(62)	3.9	
1	R1Pc10A	13000	(58)	114.3	
1	R1Pc3A	12000	(53)	550.	
1	R1Pc8A	10000	(44)	-	a
2	R2Pc5C	14000	(62)	22.2	
2	R2Pc10A	13000	(58)	47.6	
2	R2Pc4A	12000	(53)	37.3	
2	R2Pc10B	11000	(49)	76.9	
2	R2Pc6B	10000	(44)	92.8	
3	R3Pc1B	11000	(49)	2.6	
3	R3Pc4B	10000	(44)		b
3	R3Pc2B	10000	(44)	29.6	
4	R4Pc7A	11000	(49)	0.3	
4	R4Pc7B	10000	(44)	8.3	
5	R5APc8	12000	(53)	27.9	
5	R5APc6A	11000	(49)	21.0	b
5	R5APc6A	11000	(49)	424.	c
5	R5APc6B	11000	(49)	172.6	
5	R5APc3A	10000	(44)	180.4	
6	R6Pc8B	13000	(58)	4.8	
6	R6Pc9	12000	(53)	57.4	d
6	R6Pc5A	11000	(49)	114.4	e,f
6	R6Pc1A	10000	(44)	169.6	
7	R7Pc1	12000	(53)	0.8	
7	R7Pc3A	11000	(49)	73.0	e
7	R7Pc2A	10000	(44)	66.0	

Continued

TABLE A.3 - (Continued)

Run No.	Specimen No.	Test load lbf	(kN)	Time to rupture h	Notes
8	R8Pc3B	11000	(49)	0.08	
8	R8Pc1B	10000	(44)	0.2	
9	R9Pc1B	13000	(58)	0.05	
9	R9Pc2B	12000	(53)	2.2	
9	R9Pc9B	11000	(49)	26.5	
9	R9Pc3B	10000	(44)	13.3	
9	R9Pc10A	10000	(44)	20.0	
10	R10Pc3B	13000	(58)	2.0	
10	R10Pc2B	12000	(53)	28.4	
10	R10Pc4B	11000	(49)	450.	g
11	R11Pc13A	14000	(62)	0.3	
11	R11Pc4A	13000	(58)	168.	
11	R11Pc11A	12000	(53)	25.6	d
11	R11Pc19A	11000	(49)	0.00	b
11	R11Pc20A	11000	(49)	214.5	
11	R11Pc9A	11000	(49)	293.3	d
11	R11Pc15	10000	(44)	67.7	
11	R11Pc3	10000	(44)	123.4	h

Notes:

a. Test discontinued after 1000h without failure.
b. Specimen pulled out of end fitting.
c. Same as specimen above. Ends repotted. Sustained 402.8h additional before failure.
d. Failure initiated at or in end fitting.
e. Test interrupted by 3-day power outage during which load was maintained but temperature and humidity decreased to ambient. This interval not included in time to rupture.
f. ±7.5h; timer failed to function properly.
g. ±25h; timer failed to function properly.
g. ±12.2h; timer failed to function properly.

TABLE A.4

RESULTS OF STRESS-RUPTURE TESTS AT 160°F (71°C) and SATURATED HUMIDITY, RUNS 1-11

Rod diameter: 1/2 in (13 mm), nominal.
End fittings: Type R/P with cruciform wedges and C2W3 potting compound.
All failures occurred in the free length within the temperature-humidity chamber, except as noted.

Run No.	Specimen No.	Test load lbf	(kN)	Time to rupture h	Notes
1	R1Pc1A	13000	(58)	0.6	
1	R1Pc2B	12000	(53)	5.1	
1	R1Pc2A	11000	(49)	148.1	
1	R1Pc1B	10000	(44)	83.4	
1	R1Pc4B	10000	(44)	229.2	
1	R1Pc7A	10000	(44)	270.7	a
2	R2Pc8	13000	(58)	0.2	
2	R2Pc2	13000	(58)	0.8	
2	R2Pc6A	12000	(53)	49.4	
2	R2Pc3A	11000	(49)	362.	
2	R2Pc3B	10000	(44)	480.	
3	R3Pc9A	10000	(44)	0.7	
3	R3Pc3A	10000	(44)	4.6	
4	R4Pc9	10000	(44)	2.3	
5	R5APc5	13000	(58)	3.3	
5	R5APc8B	12000	(53)	167.	b
5	R5APc2A	11000	(49)	780.	c
5	R5APc3B	10000	(44)	444.	
6	R6Pc8A	13000	(58)	6.2	
6	R6Pc6B	12000	(53)	80.8	
6	R6Pc5B	11000	(49)	540.	
6	R6Pc1B	10000	(44)	599.	
7	R7Pc4	12000	(53)	2.0	d
7	R7Pc3B	11000	(49)	114.4	e
7	R7Pc2B	10000	(44)	418.	
8	R8Pc2B	10000	(44)	0.5	

Continued

TABLE A.4 - (Continued)

Run No.	Specimen No.	Test load lbf	(kN)	Time to rupture h	Notes
9	R9Pc8B	11000	(49)	0.07	
9	R9Pc8A	11000	(49)	0.5	
9	R9Pc10B	10000	(44)	847.	
10	R10Pc8	12000	(53)	2.0	
10	R10Pc6A	12000	(53)	46.7	f
10	R10Pc5A	11000	(49)	241.5	
10	R10Pc5B	10000	(44)	411.	
11	R11Pc8A	13000	(58)	22.9	
11	R11Pc17	12000	(53)	94.7	
11	R11Pc18	11000	(49)	145.5	
11	R11Pc12	10000	(44)	509.	e
11	R11Pc6	10000	(44)	600.	e

Notes:

a. $\pm$9.5h; timer failed to function properly.
b. $\pm$7.5h; timer failed to function properly.
c. Test interrupted by 3-day power outage during which load was maintained but temperature and humidity decreased to ambient. This interval not included in time to rupture.
d. Failure initiated at surface blemish on specimen.
e. Failure initiated at or in end fitting.
f. Specimen pulled out of end fitting.

TABLE A.5

RESULTS OF CONVENTIONAL TENSILE TESTS, RUNS 12 AND 13

Rod diameter: 1/2 in (13 mm), nominal.
Free length: 52 to 62 in (1.3 to 1.6 m), except as noted.
Crosshead speed: 0.75 in/min (0.32 mm/s).
End fittings: H3M with cruciform wedges and C2W3 potting compound.

Run No.	Specimen No.	Maximum load lbf	(kN)	Notes
12	R12Pc16	23750	(106)	a
12	R12Pc17	25750	(115)	b
12	R12Pc18	24250	(108)	a
12	R12Pc2A	26750	(119)	a,c
12	R12Pc2B	24700	(110)	a,c
13	R13Pc16	23950	(107)	a
13	R13Pc17	25000	(111)	a
13	R13Pc18	24400	(109)	a
13	R13Pc2B	25250	(112)	a,c
13	R13Pc2C	23750	(106)	a,c

Notes:

a. Failed in end fitting following delamination.

b. Failed in free length following delamination.

c. Free length, 23 to 26 in (0.6 to 0.7 m).

TABLE A.6

RESULTS OF HIGH-SPEED TENSILE TESTS, RUNS 12 AND 13

Rod diameter: 1/2 in (13 mm), nominal.
Free length: 27 to 28 in (0.7 m).
Crosshead speed: 300 in/min (130 mm/s).
End fittings: H3M with cruciform wedges and C1W2 potting compound.
All failures appeared to have initiated in an end fitting.

Run No.	Specimen No.	Maximum load	
		lbf	(kN)
12	R12Pc9A	32600	(145)
12	R12Pc15A	34500	(153)
13	R13Pc6A	33000	(147)

TABLE A.7

RESULTS OF STRESS-RUPTURE TESTS UNDER SATURATED HUMIDITY, RUNS 12 AND 13

Rod diameter: 1/2 in (13 mm), nominal.
End fittings: Type R/P with cruciform wedges and C2W3 potting compound.
All failures occurred in the free length within the temperature-humidity chamber, except as noted.

Run No.	Specimen No.	Temperature		Test load		Time to rupture	Notes
		°F	(°C)	lbf	(kN)	h	
12	R12Pc11	200	(93)	13000	(58)	2.4	a
12	R12Pc4	200	(93)	12000	(53)	190.1	
12	R12Pc13	200	(93)	11000	(49)	568.	
12	R12Pc14	160	(71)	13000	(58)	4.3	a
12	R12Pc12	160	(71)	12000	(53)	165.7	
12	R12Pc1	160	(71)	11000	(49)	233.4	b
12	R12Pc5	160	(71)	11000	(49)	320.	
13	R13Pc9	200	(93)	12000	(53)	24.9	
13	R13Pc5	200	(93)	11000	(49)	96.0	
13	R13Pc1	200	(93)	10000	(44)	400.	
13	R13Pc3A	160	(71)	12000	(53)	0.8	
13	R13Pc15	160	(71)	11000	(49)	220.8	
13	R13Pc12	160	(71)	10000	(44)	804.	

Notes:

a. Delaminated prior to failure.

b. Failure initiated at end fitting.

TABLE A.8

RESULTS OF CONVENTIONAL TENSILE TESTS ON PRELIMINARY SAMPLE OF ARAMID/ISOPHTHALIC ROD

Rod diameter: 1/4 in (6 mm), nominal.
Crosshead speed: 0.75 in/min (0.32 mm/s).
End fittings: As listed, with cruciform wedges for the H3M and Type R/P fittings, and C2W3 potting compound except as noted.

Specimen No.	End fitting	Maximum load		Notes
		lbf	(kN)	
22A	R/P	6600	(29)	a
22B	R/P	6500	(29)	a
22C	Mod 4	6850	(30)	b
22D	Mod 4	7050	(31)	b,c
22E	H3M	6750	(30)	d
22F	H3M	3500	(16)	b,e

Notes:

a. Specimen failed adjacent to fitting.

b. Specimen pulled out of fitting.

c. Mod 4 end fitting was modified to provide additional potted length.

d. C1W1 potting compound was used. Specimen failed inside fitting.

e. PC8 potting compound was used.

TABLE A.9

RESULTS OF CONVENTIONAL TENSILE TESTS, RUNS 14 AND 15

Rod diameter: 1/2 in (13 mm), nominal.
Free length: 47 to 48 in (1.2 m).
Crosshead speed: 0.75 in/min (0.32 mm/s).
End fittings: H3M with cruciform wedges and C2W3 potting compound, except as noted.

Run No.	Specimen No.	Maximum load lbf	(kN)	Notes
14	R14Pc3	25850	(115)	a
14	R14Pc10	28750	(128)	b
14	R14Pc20	28050	(125)	a
14	R14APc1	24450	(109)	b,c
15	R15Pc2	27650	(123)	a
15	R15Pc18	25650	(114)	a
15	R15Pc20	26950	(120)	a
15	R15Pc3	11750	(52)	a,d
15	R15Pc24	17450	(77)	e,f
15	R15Pc21	22250	(99)	e,g
15	R15Pc1	10600	(47)	e,h
15	R15Pc7	23450	(104)	a,i

Notes:

a. Specimen failed inside end fitting.
b. Specimen failed in free length.
c. Specimen pultruded at 12 in/min (5 mm/s) rather than 6 in/min (3 mm/s); poor surface quality
d. Aramid fibers broomed out in fitting before potting.
e. Specimen pulled out of end fitting.
f. Reduced length of potting cavity in fitting.
g. Enlarged diameter of potting cavity in fitting.
h. Used Type P end fittings [5].
i. Specimen subjected to stress-rupture test (Table A.11) before tensile test; Type R/P end fittings.

TABLE A.10

RESULTS OF HIGH-SPEED TENSILE TESTS, RUNS 14 & 15

Rod diameter: 1/2 in (13 mm), nominal.
Free length: 27 to 28 in (0.7 m).
Crosshead speed: 300 in/min (130 mm/s).
End fittings: H3M with cruciform wedges and C1W2 potting compound.

Run No.	Specimen No.	Maximum load lbf	(kN)	Notes
14	R14Pc1	35000	(156)	a
15	R15Pc3	28000	(125)	b
15	R15Pc22	30000	(133)	a

Notes:

a. Specimen failed in free length.

b. Specimen failed inside end fitting.

TABLE A.11

RESULTS OF STRESS-RUPTURE TESTS UNDER SATURATED HUMIDITY, RUNS 14 & 15

Rod diameter: 1/2 in (13 mm), nominal.
End fittings: Type R/P (except as noted) with cruciform wedges and C2W3 potting compound.

Run No.	Specimen No.	Temperature F	(C)	Test load lbf	(kN)	Time to rupture h	Notes
14	R14Pc17	200	(93)	13000	(58)	22.3	a
14	R14Pc5	200	(93)	12000	(53)	147.5	a
14	R14Pc13	200	(93)	11000	(49)	218.6	a,b
14	R14Pc14	200	(93)	10000	(44)	591.0	a
14	R14Pc12	160	(71)	14000	(62)	1.6	a
14	R14Pc2	160	(71)	13000	(58)	4.6	a
14	R14Pc19	160	(71)	13000	(58)	417.3	a,c
14	R14Pc15	160	(71)	12000	(53)	393.3	a
14	R14Pc6	160	(71)	11000	(49)	462.5	a
14	R14Pc17	160	(71)	10000	(44)	324.9	a
14	R14Pc18	160	(71)	10000	(44)	668.0	a
15	R15Pc13	200	(93)	16000	(71)	18.6	a
15	R15Pc6	200	(93)	14000	(62)	328.8	b
15	R15Pc11	200	(93)	14000	(62)	260.6	a
15	R15Pc12	200	(93)	12000	(53)	548.0	a
15	R15Pc15	160	(71)	16000	(71)	351.4	b,d
15	R15Pc14	160	(71)	16000	(71)	0.2	d,e
15	R15Pc17	160	(71)	16000	(71)	118.6	a,e
15	R15Pc8	160	(71)	14000	(62)	470.9	a
15	R15Pc4	160	(71)	14000	(62)	738.3	a
15	R15Pc7	160	(71)	12000	(53)	-	f

Notes:

a. Specimen failed in free length within temperature-humidity chamber.
b. $\pm$7.5 h; timer malfunctioned.
c. $\pm$10.0 h; timer malfunctioned.
d. Specimen failed inside end fitting.
e. Used H3M end fittings.
f. Test discontinued after 2004 h without failure.

ADDENDUM

A SPECIFICATION FOR ARAMID FRP ROD

Leonard Mordfin

In the main text of this report it was shown that, in spite of its promise of superior weatherability, aramid FRP rod cannot be recommended for service in antenna-support applications without further study. Nevertheless, based upon the data and information acquired in the program, this addendum contains a basic specification and briefly discusses certain aspects of its preparation.

The data and information acquired in the program were to limited for the preparation of a thorough, all-inclusive specification. This is due, in large measure, to the fact that fatigue tests and real-time outdoor weathering tests, which were originally intended to be performed in the present program, were later cancelled due to budgetary limitations. Three approaches were explored in an attempt to overcome this paucity of well-characterized data. First, some data from other sources were used (e.g., [5,35]). Second, some requirements gleaned from specifications for glass FRP rod were included in the present document where they were considered to be applicable. These other specifications, which were found to be extremely helpful, include the following:

> Military Specification MIL-P-79C, Plastic Rods and Tubes, Thermosetting, Laminated (15 June 1961, amended 10 Sept. 1964).

Specification No. IBS/ET-426, Antenna Guy Lines and Insulators - Fiberglass Rods, U.S. Information Agency (Washington, revised Dec. 4, 1974).

BPA Specification ETF 50-03.2, Technical Specification for Fiber Glass Strain Insulators, Bonneville Power Administration (Portland, Ore., July 10, 1972).

NAVFAC Specification No. 21-71-0900, Procurement of Fiberglass Rod Insulators for the U.S. Naval Radio Station, Totsuka, Japan, Naval Facilities Engineering Command (Washington, Aug. 10, 1972).

Despite this additional information some serious gaps still remain. For example, virtually nothing appears to be known about the flexural strength of aramid FRP rod; and testing for the reported tendency of organic fibers like PRD, Nylon etc to creep under tensile stresses was not specifically conducted. Therefore these conditions appear as applied field blank spaces in the present specification. Also, the present specification does not address quality assurance requirements such as dimensional tolerances and unacceptable surface defects. In this area, fortunately, help is on the way. Guidelines for these characteristics of pultruded rod are presently being developed under the jurisdication of ASTM Section D20.18.02.

The third approach taken, in the effort to make the specification sufficiently rigorous, was to include both material and fabrication requirements and performance requirements. There is a philosophy, to which this author subscribes, that the inclusion of both of these types of requirements in the same specification tends to produce a redundant and unecessarily restrictive document. It will be noted, however, that an attempt was made, in the specification which follows, to avoid these pitfalls through the use of suitable "escape" clauses. Nevertheless, it must not be inferred that this specification is endorsed by the National Bureau of Standards.

* * *

Draft Technical Specification
for
WEATHER-RESISTANT NONMETALLIC STRUCTURAL ROD

1. SCOPE. This specification governs the technical requirements for weather-resistant, nonmetallic rods intended for use in research and evaluative programs with ultimate applications in antenna-support systems.

2. APPLICABLE DOCUMENTS. The most recent editions of the following documents of the American Society for Testing and Materials form a part of this specification to the extent specified herein.

D 149 Tests for Dielectric Breakdown Voltage and Dielectric Strength of Electrical Insulating Materials at Commercial Power Frequencies

D 257 Tests for D-C Resistance or Conductance of Insulating Materials

D 785 Test for Rockwell Hardness of Plastics and Electrical Insulating Materials

D 2343 Test for Tensile Properties of Glass Fiber Strands, Yarns, and Rovings Used in Reinforced Plastics

D 2344 Test for Apparent Horizontal Shear Strength of Reinforced Plastics by Short Beam Method

3. GENERAL REQUIREMENTS. The rods shall be composed of unidirectional aramid fiber rovings impregnated with a high quality, weather-resistant resin binder, and shall be fabricated by the pultrusion process. All of the rovings shall be continuous throughout each length of rod. The rods shall have smooth exterior surfaces which resist contamination. No coating is required on the exterior surfaces. However, if a coating other than an integral gel coating is applied to the exterior surfaces

then it shall be demonstrable that the rods satisfy all of the requirements of this specification in both the coated and the uncoated conditions except as specifically noted herein.

The rods shall have a circular cross section. The lengths and the diameters of the rods shall be as specified in the applicable procurement document. Rods of lengths less than 10 ft (3.0 m) shall be furnished in the straight condition. Rods of greater length may be furnished in a coiled condition.

4. MATERIALS REQUIREMENTS.

4.1 Reinforcing material. The reinforcing material for the rods shall be continuous aramid fiber roving of commercial grade or better, certified by its manufacturer to be suitable for aircraft and commercial tape and filament-winding applications. The fibers shall have a nominal diameter of 0.00046 in (0.012 mm). The roving shall have an end count (number of strands per roving) of not less than 10, with not less than 1000 fibers per strand. The mechanical properties of the roving shall be certified by its manufacturer to meet or exceed the following average requirements, determined in accordance with the test procedures specified in ASTM D 2343 for glass fiber roving:

Tensile strength, 500 000 lbf/in^2 (3400 MPa).
Tensile modulus of elasticity, 19 x 10^6 lbf/in^2 (130 GPa).

Except as noted in Paragraph 4.4, the roving shall not contain any surface finish or sizing, nor any grease, oil, dirt or other foreign matter. It shall not contain knots or excessive loose fibers or fuzz which reduce the smoothness of the roving.

4.2 Resin binder material. Except as noted in Paragraph 4.4, the resin binder material for the rods shall consist primarily of propoxylated bisphenol-A polyester resin.

4.3 Coating material. A coating may be added to the exterior surfaces of the rods to enhance weatherability. If used, it shall be primarily organic although it may contain inorganic ingredients. The coating shall be applied uniformly over the surfaces of the rods to a thickness not exceeding 0.10 in (2.5 mm). The coating shall be flexible, well-adhered, and resistant to peeling and flaking.

4.4 Exceptions. A surface finish, sizing or coupling agent may be used on the aramid fiber roving in order to facilitate its impregnation with the resin binder, provided that the provisions of Paragraph 4.4.1 are met.

A high quality, weather-resistant, thermosetting polyester resin other than that specified in Paragraph 4.2 may be used in order to facilitate the impregnation of the rovings, or to enhance the weatherability of the rods, or both, provided that the provisions of Paragraph 4.4.1 are met.

4.4.1 If a surface finish, sizing or coupling agent is used on the rovings or if a resin binder other than that specified in Paragraph 4.2 is used, or both, then it shall be demonstrable that the horizontal shear strength of the rod, in the axial direction, is not less than 6200 lbf/in^2 (43 MPa). This demonstration shall be made in accordance with ASTM D 2344 using flat test specimens machined from the pultruded rod.

5. FABRICATION REQUIREMENTS. Fabrication of the rods shall be carried out by skilled craftsmen using the best modern practices of the pultrusion industry.

5.1 The rovings shall be dried, for not less than 8h at not less than 250°F (120°C), immediately prior to pultrusion. They shall be maintained in the dry condition by passing them through a suitable heating chamber until immersion in the resin trough is effected.

5.2 The quantity of roving to be used shall be sufficient to provide a fiber content, in the rod product, of not less than 56 percent by weight (mass). This fiber content shall be verifiable by means of the following formula:

$$\text{Fiber content} = \frac{\text{Weight (mass) of a unit length of roving}}{\text{Weight (mass) of a unit length of rod}} \times \text{Number of rovings used.}$$

5.3 The resin binder formulation shall consist of the resin specified in Paragraph 4, thinned with the minimum concentration of monostyrene necessary to provide a sufficiently low viscosity for satisfactory impregnation and pultrusion. The formulation shall also contain the required catalyst concentration and an ultraviolet inhibitor to enhance the weatherability of the rod product. The formulation may also contain a die lubricant to facilitate pultrusion. The formulation shall not contain a wetting agent or a coupling agent nor any grease, oil, dirt or other foreign matter.

5.4 The pulling speed and the curing temperature profile shall be selected to produce a well-cured product with good surface quality.

5.5 The immersion time, defined as the immersed length of roving in the resin trough divided by the pulling speed, shall not exceed 4 min.

5.6 All rods of length not exceeding 10 ft (3.0 m) shall be post cured for not less than 15h at 275°F (135°C). The rods shall be fully supported during post curing to avoid warping.

5.7 Coiling of the rod product, when necessary, shall not be attempted until it has cooled to 100°F (38°C) or less, and shall be carried out with extreme care to assure that no portion of the rod is bent, even momentarily, to a radius of curvature which is less than half the coil diameter. The coil diameter shall be not less than 300 times the rod diameter unless the provisions of Paragraph 6.5 are met.

6. PERFORMANCE REQUIREMENTS

6.1 Tensile strength. The rods shall be capable of sustaining a tensile stress of not less than 125,000 lbf/in^2 (860 MPa) for not less than one minute without visible or audible damage or other evidence of incipient failure. This shall be demonstrable by tensile tests on full cross-section rods, of lengths not less than 100 times the rod diameter, to which high-performance end fittings have been attached. A mechanical failure of the rod specimen which initiates in an end fitting prior to the completion of the one-minute interval shall render the test invalid but shall not in itself disqualify the product.

6.2 Stress-rupture strength. The rods shall be capable of sustaining a tensile stress of not less than 70,000 lbf/in^2 (480 MPa) for not less than 240 h while exposed, in an environmental test chamber, to a temperature of $160 \pm 5^{\circ}$F ($73 \pm 3^{\circ}$C) and saturated-humidity conditions. This shall be demonstrable by tensile stress-rupture tests on full cross-section rods to which suitable end fittings have been attached. The length of rod exposed to the specified environment shall be not less than 50 times the rod diameter but the end fittings need not be so exposed. At the completion of the test the rod shall exhibit no evidence of structural damage or deterioration or other evidence of incipient failure. A mechanical failure of the rod specimen which initiates in an end fitting prior to the completion of the 240-h interval shall render the test invalid but shall not in itself disqualify the product.

6.3 Flexural Strength. When specified, the flexural strength of the rods shall be not less than (*)

at room temperature, and not less than 90 percent of this value at a temperature of -70°F (-57°C). This shall be demonstrable by three-point bending tests on full cross-section rods, at room temperature and at -70°F (-57°C), using a span-to-diameter ratio of 36 to 40.

6.4 Fatigue Strength. When specified, the rods shall be capable of sustaining aeolian vibration indefinitely. This shall be demonstrable by means of tests in which full cross-section rods, of lengths not exceeding 600 times the rod diameter, are subjected to transverse vibration at a resonant frequency between 45 and 90 Hz while under an axial tensile stress of not less than 70 000 lbf/in^2 (480 MPa). The double amplitude of vibration shall be not less than three times the rod diameter. Rod specimens so tested shall be capable of enduring not less than 10^8 cycles of vibration without evidence of damage.

6.5 Storage Capability. Rods may be coiled to diameters less than those specified in Paragraph 5.7 provided that the storage capability of the coiled rods is not thereby degraded. This shall be demonstrable by means of tests in which coils of full cross-section rod, consisting of not less than three full loops per coil, are exposed to a temperature of not less than 200°F (93°C) for not less than 72 h. Rod material so tested shall exhibit no evidence of buckling or other structural damage and, upon uncoiling, shall not retain excessive permanent set.

(*) See text under the ADDENDUM

6.6 Hardness. The exterior surfaces of post-cured rods shall exhibit an average hardness number of not less than 30 on the Rockwell E scale. In the case of coated rods this requirement shall apply only to the rods in the uncoated condition. This performance requirement shall be demonstrable by means of measurements performed in accordance with Procedure A of ASTM D 785.

6.7 Electrical resistance. The insulation resistance of the rods shall be not less than 10^{15} ohms per inch (40,000 TΩ/m) of length. This shall be demonstrable by means of measurements performed in accordance with ASTM D 257 using a direct voltage of not less than 500 V.

6.8 Dielectric strength. Rod samples shall exhibit average dielectric strengths, in the axial direction, of not less than 70 V/mil (2.8 MV/m) in the dry condition and 15 V/mil (0.6 MV/m) immediately after immersion for 2 h in boiling distilled water. This shall be demonstrable on full cross-section samples having lengths equal to the rod diameter by means of tests performed in oil in accordance with the short-time test procedure of ASTM D 149 using a rate-of-rise of 500 V/s at a frequency of 60 Hz.

7. QUALITY ASSURANCE REQUIREMENTS

(The level of experience acquired to date, on material of the kind specified herein, is inadequate for the establishment of firm requirements at this time for dimensional tolerances, acceptable surface defects, etc.)

1. Morrison, R. S., Pultrusion, Modern Plastics Encyclopedia 1973-1974, ed. S. Gross, pp 428-431 (McGraw-Hill, N.Y., 1973).

2. Mohr, J. G., Oleesky, S. S., Shook, G. D. and Meyer, L. S., Pultrusion and Rod Stock, Chap. V-2 in SPI Handbook of Technology and Engineering of Reinforced Plastics/Composites, 2nd Ed., pp 269-276 (Van Nostrand Reinhold, N.Y., 1973).

3. Anon., Pultrusion Process Puts Glass Fibers in One Direction for High Strength, Product Engineering 44, No. 11, pp 38-40 (Nov. 1973).

4. Chwirut, D. J. (coordinator), Research and Testing Facilities of the Engineering Mechanics Section, National Bureau of Standards, Washington, D. C., NBS Spec Publ 370 (1973).

5. Halsey, N., Mitchell, R. A., and Mordfin, L., Evaluation of GRP Rod and Rope Materials and Associated End Fittings, NBS Report IR 73-129 (Dec. 1972).

6. Anon., Standard Method of Test for Ignition Loss of Cured Reinforced Resins, ASTM Designation D 2584-68, 1975 Annual Book of ASTM Standards, Part 36 (Am Soc Test Mat, Philadelphia, 1975).

7. Anon., Specific Gravity from Weight and Volume Measurements, Method 5012, Plastics: Methods of Testing, Fed. Test Method Std. No. 406 (General Services Administration, Washington, Oct. 5, 1971).

8. Hudock, J. A., private communication.

9. Anon., Standard Method of Test for Rockwell Hardness of Plastics and Electrical Insulating Materials, ASTM Designation D 785-65, 1975 Annual Book of ASTM Standards, Part 35, loc. cit.

10. Anon., Standard Method of Test for Splitting Tensile Strength of Cylindrical Concrete Specimens, ASTM Designation C 496-71, 1975 Annual Book of ASTM Standards, Part 14, loc. cit.

11. Mordfin, L., and Kerper, M. J., Strength Testing of Ceramics - A Survey, Mechanical and Thermal Properties of Ceramics, ed. J. B Wachtman, Jr., NBS Spec Publ 303, pp 243-262 (1969).

12. Aitchison, C. S., and Miller, J. A., A Subpress for Compressive Tests, NACA TN 912 (1943).

13. Halsey, N., Properties of Glass Fiber-Reinforced Polymers for Application to Guy-Insulator Systems of Communication Towers, Phase 2, Test Methods and Evaluations of Glass Fiber-Reinforced Polymer Rods for Use in Guy-Insulator Systems of Loran C. Towers, NBS Report 10261 (June 1970).

14. Mitchell, R. A., Woolley, R. M., and Halsey, N., High-Strength End Fittings for FRP Rod and Rope, J. Engineering Mechanics Div. ASCE 100, No. EM4, pp 687-706 (Aug. 1974).

15. Mitchell, R. A., Woolley, R. M. and Fisher, C. R., Formulation and Experimental Verification of an Axisymmetric Finite-Element Structural Analysis, J. Res. NBS 75C3&4-322, pp 155-163 (1971).

16. Marlowe, D. E., Halsey, N., Mitchell, R. A. and Mordfin L., Non-Metallic Antenna-Support Materials, First Annual Interim Report, NBS Report IR 73-233 (April 1973).

17. Mitchell, R. A., Woolley, R. M., and Chwirut, D. J., Analysis of Composite-Reinforced Cutouts and Cracks, AIAA J 13, No. 6, pp 744-749 (June 1975).

18. Anon., Standard Method of Test for Tensile Properties of Glass Fiber Strands, Yarns, and Rovings Used in Reinforced Plastics, ASTM Designation D 2343-67, 1975 Annual Book of ASTM Standards, Part 36, loc. cit.

19. Anon., Suggested SPI Procedure - Procedure for Running Exotherm Curves Using the Block Test Method, Proc. SPI Reinforced Plastics/Composites Division, Washington, Feb. 1969, 24th Annual Conference (Society of the Plastics Industry, N.Y., 1969).

20. Titus, J. B., New Plastics: Properties, Processing and Potential Uses, Plastic Special Report 9 (Plastics Technical Evaluation Center, Picatinny Arsenal, Dover, N. J., May 1971).

21. Lundberg, R. D., Koleske, J. V., and Walter, E. R., Dispersing Aids for Particulate Solids, Canadian Patent No. 866261 (Mar 16, 1971).

22. Atkins, K. E., Harpold, M. A., Comstock, L. R., and Smith, P. L., Vinyl Polymers and -Caprolactone Polymers as Low Profile Additives, Proc. SPI Reinforced Plastics/Composites Institute, Washington, Feb 1973, 28th Annual Conference, Paper No. 1-B, loc. cit.

23. Browning, C. E., and Hartness, J. T., Effects of Moisture on the Properties of High-Performance Structural Resins and Composites, in Composite Materials: Testing and Design (Third Conference), C. A. Berg, F. J. McGarry and S. Y. Elliott, coordinators, ASTM STP 546, pp 284-302 (1974).

24. Ishai, O., and Mazor, A., The Effect of Environmental-Loading History on Longitudinal Strength of Glass-Fiber Reinforced Plastics, Rheologica Acta 13, No. 3, pp 381-394 (1974).

25. Brunauer, S., The Adsorption of Gases and Vapors, Volume 1, Physical Adsorption, p 14 (Princeton University Press, 1945).

26. Glasstone, S., and Lewis, D., Elements of Physical Chemistry, 2nd ed., p 559 (D. Van Nostrand Co., Princeton, N.J., 1960).

27. Halsey, N., Marlowe, D. E., and Mordfin, L., Non-Metallic Antenna-Support Materials, Second Annual Interim Report, NBS Report IR 74-557 (June 1974).

28. Chiao, T. T., and Moore, R. L., Organic-Fiber/Epoxide Composites, Composites 4, No. 1, pp 31-33 (England, 1973).

29. Chiao, T. T., Wells, J. E., Moore, R. L., and Hamstad, M. A., Stress-Rupture Behavior of Strands of an Organic Fiber/Epoxy Matrix, in Composite Materials: Testing and Design (Third Conference), pp 209-224, loc. cit.

30. Readdy, A. F., and Holman, B. T., Resistance of Plastics to Outdoor Weathering, Addendum No. 6 to Technical Report 2102 (Picatinny Arsenal, Dover, N.J., June 1967).

31. Alumbaugh, R. L., and Roe, T., Jr., Reinforced Plastics Laminates Panels -- Physical Tests of Panels Removed after the Fourth Exposure Period, Technical Note N-1084 (Naval Civil Engineering Laboratory, Port Hueneme, Calif., Mar 1970).

32. Yeoman, F. A., et al, private communication.

33. Hoggatt, J. T., Development of Cryogenic PRD-49-1 Filament-Wound Tanks, NASA CR-120835 (Boeing Co., Seattle, Dec 1971).

34. Rhodehamel, J. R., private communication.

35. Sturgeon, D. L., Wolffe, R. A., Miner, L. H., and Wagle, D. G., PRD-49 Fiber & Composite Performance, E. I. du Pont de Nemours & Co., Inc., Textile Fibers Dept. (Wilmington), revised June 5, 1972.

36. Kulkarni, S. V., Rice, J. S., and Rosen, B. W., An Investigation of the Compressive Strength of PRD-49-III/Epoxy Composites, NASA CR-112334 (Materials Sciences Corp., Blue Bell, Pa., undated).

37. Dickard, H. E., Williams, R. T., Banuk, R. E., et al, Design and Fabrication of an RPV Wing Panel with PRD-49/Epoxy Skins, AFFDL-TR-73-31 (Mar 1973).

38. Pritchard, G., and Taneja, N., Nature and Extent of Water Damage in Glass Laminates, Proc. SPI Reinforced Plastics/Composites Institute, Washington, Feb 1974, 29th Annual Conference, Paper No. 2-C, loc. cit.

UNCLASSIFIED

SECURITY CLASSIFICATION OF THIS PAGE (When Data Entered)

REPORT DOCUMENTATION PAGE		READ INSTRUCTIONS BEFORE COMPLETING FORM
1. REPORT NUMBER AFML-TR-76-42	2. GOVT ACCESSION NO.	3. RECIPIENT'S CATALOG NUMBER
4. TITLE (and Subtitle) NON-METALLIC ANTENNA-SUPPORT MATERIALS PULTRUDED RODS FOR ANTENNA GUYS, CATENARIES AND COMMUNICATIONS STRUCTURES		5. TYPE OF REPORT & PERIOD COVERED Final Technical Report 6. PERFORMING ORG. REPORT NUMBER NBSIR 75-684
7. AUTHOR(s) N. Halsey R. A. Mitchell D. E. Marlowe L. Mordfin		8. CONTRACT OR GRANT NUMBER(s) D.O. F33615-72-M-5000
9. PERFORMING ORGANIZATION NAME AND ADDRESS National Bureau of Standards Washington, D.C. 20234		10. PROGRAM ELEMENT, PROJECT, TASK AREA & WORK UNIT NUMBERS
11. CONTROLLING OFFICE NAME AND ADDRESS		12. REPORT DATE May 1976 13. NUMBER OF PAGES
14. MONITORING AGENCY NAME & ADDRESS(if different from Controlling Office)		15. SECURITY CLASS. (of this report) Unclassified 15a. DECLASSIFICATION/DOWNGRADING SCHEDULE

16. DISTRIBUTION STATEMENT (of this Report)

Approved for public release; distribution unlimited.

17. DISTRIBUTION STATEMENT (of the abstract entered in Block 20, if different from Report)

18. SUPPLEMENTARY NOTES

19. KEY WORDS (Continue on reverse side if necessary and identify by block number)

Aramid
Glass
Composite Materials
Fiber-reinforced-plastic (FRP)
End-fittings for FRP rod
Environmental resistance of FRP rods
Guys, antenna
Pultrusion
Reinforced plastics
Stress rupture of FRP rod
Test methods
Weatherability of FRP rods

20. ABSTRACT (Continue on reverse side if necessary and identify by block number)

Both E-glass and Kevlar 49 (aramid) fibers were used to reinforce an isophthalic polyester resin. These materials were used, in turn, to form pultruded antenna rod hardware for structural tests. The aramid material exhibited substantially improved strength-retention properties over the glass-reinforced material under prolonged exposure to heat and humidity. The aramid material offers the promise of superior weatherability in antenna-support applications although further testing is warranted. The stress-rupture properties of pultruded rod, under high humidity, possess unusual

DD FORM 1 JAN 73 1473 EDITION OF 1 NOV 65 IS OBSOLETE

UNCLASSIFIED

SECURITY CLASSIFICATION OF THIS PAGE (When Data Entered)

20. Abstract (Continued)

temperature and time dependencies. These are explained in terms of the mechanisms whereby moisture is transported from the environment to the fiber/matrix interface. The stress-rupture properties, as well as the tensile properties, may be improved by appropriately modifying the pultrusion process.

Two new end fittings, generally capable of attaining the full tensile strength of glass fiber-reinforced pultruded rod, were developed.

Several new test methods were developed, including an environmental stress-rupture test, two methods for investigating the quality of the fiber/matrix interface, and a method for examining the rate sensitivity of the tensile strength. A significant rate sensitivity was observed for glass fiber-reinforced rod but not for aramid fiber-reinforced rod.